Universidad
Carlos III de Madrid

NATURAL FIBERS BASED ARMOUR SOLUTIONS TO COUNTER IMPROVISED EXPLOSIVE DEVICES

Tutor: Carlos Santiuste Romero
Student: Dragos Gabriel Nedelcu
Bachelor's Degree in Aerospace Engineering

Abstract

This paper discusses the blast response of walls reinforced with biodegradable materials and the viability of this solution. Intentional or accidental blast can affect military and civilian buildings. Besides the production of deadly fragments as a result of the strain energy accumulated by the structure, blasts can also lead to the collapse of the whole building. The existing solutions such as Kevlar reinforcements are expensive, not easy to deploy and not environmentally friendly. Due to their ecofriendly nature and sustainability, Natural Fiber Composites are getting a lot of attention from researchers lately. The properties of these materials are widely varied depending on factors such as the type of fiber and source or the structure of the fibers. However, NFRPCs also present themselves with several drawbacks such as water absorption, viscoelastic behavior and lower mechanical properties. This paper has a special focus on the structural properties and whether NFRPCs represent a good fit for our solution, other properties will also be discussed with fewer details.

Natural Fiber Reinforced Polymer Composites were considered for reinforcing the walls due to their structural and biodegradable properties, costs and easiness of manufacturing. The behavior of a Natural Fiber Reinforced Polymer Composite reinforced concrete wall exposed to an accidental blast was simulated. The main purpose was analyzing the effect of the blast over the reinforced concrete wall and benchmark with its non-reinforced counterpart.

As a conclusion, this paper proves that the presence of the Natural Fiber Reinforced Composite coat absorbs more efficiently the strain energy of the structure as a result of the blast. It can effectively minimize the formation of deadly fragments of the reinforced walls and the probability of collapse of the whole structure. Even if their structural properties are inferior to their not environmentally friendly counterparts, Natural Fiber Reinforced Polymer Composites do represent a viable solution for a composite blast absorbing coat.

Special thanks to my tutor for his patience and availability through the creation of this work.

Index

1.Introduction

Most of old infrastructure has been built using the masonry construction technique and were not designed to withstand blast impact loading. Since recent events, such as the attack on the Spanish embassy in Kabul in 2015, the potential damage to civil building became a problem of interest. In this type of events, the majority of the damage inflicted it is not due to the blast itself, but due disintegration and fragmentation of the wall itself. This leads to hundreds of small wall fragments propelled at high speeds which represent a serious threat to the civil population inside and outside the building. Masonry, is among others one of the most used material for building either as main material or as infill for concrete framed walls also is the one that is most affected by this kind of blast impacts.

Therefore, understanding the behavior of masonry walls exposed to blast loading and developing sustainable and cost-effective ways of improving the resistance of the walls under this circumstances might will help to decrease the number of casualties in future hazards. Several methods for improving masonry blast resistance have been studied during the years, however the most widely used technique of retrofitting masonry walls is the use of fiber reinforced polymers as protective coats. This technique has shown significant improvement in wall's resistance.

The use of fiber reinforced polymers retrofitting has some other advantages respect other more traditional strengthening methods. Composites are light, have a high strength-to-weight ratio, corrosive resistant, relatively cheap and have an easy handling and application. However, the constant increase in public's opinion and corporate environmental sensitivity is leading to a greater consciences and a new focus on sustainability. It is no longer enough to solve problems, it must be done in a sustainable and environmentally friendly manner. This motivation together with new regulations is accelerating research into the field of Natural Fiber Reinforced Composites.

Leading experimental studies and evaluating the behavior of masonry structures under blast damage using full-scale prototypes it is expensive and even if possible will not allow us the degree of customization in terms of boundary conditions and materials that a software solution can offer.

The approach presented in this paper, consists among others of the exploration of several numerical models which have been simulated later on using common software solutions such as, ABAQUS. One of the key elements of this process was the material model that simulates the characteristics of both unreinforced and reinforced masonry walls. A good accuracy of the material model will lead to reliable results.

2. State-of-art of fiber reinforced composite materials retrofitting for protection against blast explosions

Fiber Reinforced Composites have been considered a good alternative to traditional materials such as steel due to their simplicity, cost-effectiveness and physical properties. Those materials manage to enhance the physical properties of both existing and new structural elements. Externally applied as coats using polymeric resins they lead to notable improvements in shear strength, ductility, tensile strength, ductility and stiffness meanwhile suffering from no corrosion.
FRCs also minimizes the loss of space and building disruption due to the installation together with being extremely cost effective respect to bonded steel reinforcement.

However, the research studies related with FRCs retrofitting against blast explosions it is very limited. Traditionally, due to extensive global peacetimes this research area was not representing a good incentive for researchers. The purpose of this section is to situate the reader with an updated review of the existing papers both numerical and experimental about the FRC retrofitting against blast explosions with a special focus on masonry walls.

2.1 Blast Explosions. A blast explosion is commonly defined as a sudden increase in volume and release of energy usually followed by an extreme release of gases and high temperatures. The most important parameter of a blast explosion is the peak of static overpressure of its blast wave, the variation of this value in open air can be expressed as a function of scaled distance, velocity of sound and static pressure. Depending on the physical state of the materials used they can be solid, liquid and gas. In most cases, the explosives used for civil structures damage are solid explosives. In turn, solid explosives are also categorized as primary and secondary depending on their reaction sensitivity. Commonly used materials for bombing belong are famous secondary explosives such as TNT and ANFO.

Fig. 1. Blast Explosion [1]

When a secondary solid explosive such as the ones mentioned above is detonated, it generates a high amount of gasses under a high temperature (up to 30GPa) and temperature (3000º C – 4000ºC). The continuous expansion of the generated gas forces out the already exiting volume it starts to occupy creating a blast wave of compressed air at the border of the gas volume generated containing a significant amount of the energy released during detonation. A shock wave is formed when the pressure of the blast wave is higher than the environment pressure (peak pressure or side-on over-pressure) that will keep expanding form the source of the explosion. A few moments after the explosion occurs, the pressure behind the shockwave decreases below the ambient pressure and creates a vacuum where ambient gases are starting to be pulled in.

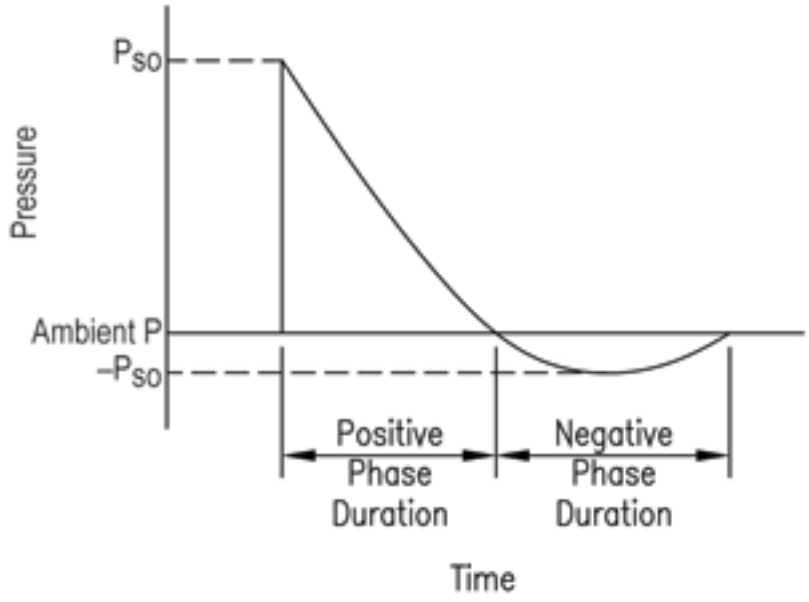

Fig. 2. Pressure variation with time during blast explosion [2]

2.2 Protection against Blast Explosions. As already mentioned at the beginning of this paper, protection for civil building became a necessity, especially public interest buildings. Materials employed for this protection work and enhancements for buildings and in order for them to be scalable solutions, they must accomplish two requirements: easiness to install and deploy and cost –effectiveness compared to traditional methods. Those materials should also be able to absorb the energy produced by the blast and avoid the collapse of the building.

Several solutions can be used in order to decrease the risk of collapse and increase protection for civilian buildings. The damage inflicted in a blast explosion can be due to the structural damage that progressively leads to the collapse of the building and due to the fragmentation (especially masonry) that breaks the wall in small fragments with high kinetic energy that become deadly.

One of the most obvious ways to decrease the damage is increasing the stand-off distance of the building using fences and walls. This translates to a lower level of incidence of the blast explosion over the building. Another traditional solution is increasing the mass of the building with extra concrete and steel which improves its structural properties. This method however can be expensive and require a long implementation.

Fig. 3. Steel stud framing [3]

Catcher systems such as steel catchers and cables can also be used to protect against fragmentation. This element can reduce the risks from ballistic shards such as glass, concrete and masonry fragments. In order to obtain a better improvement and a significant improvement in ductility, a steel stud wall can be introduced in the interior of existing walls. However, this solution has several disadvantages, such as stud failure due to strain elongation and a significant lost in floor space inside the building among high installation costs.

2.3 Fiber Reinforced Composites. Fiber Reinforced Composites have been long used in structure application with the purpose of strengthening and repair. Used to improve seismic resistance, ballistic and impact resistance or flexural strength, FRCs have many advantages such as high corrosion resistance, high durability, light weight and ease of installation and deployment. FRCs can also adapt easily to the shape of the structure. Different techniques can be used in applying FRCs to buildings, one of the most widely used being Near Surface Mounted (NSM) systems. This technique can improve significantly several structural properties such as shear properties and stiffness. Studies shown that FRCs represent a considerable improvement against blast impacts especially in masonry walls reducing fragmentation and improving the structural strength avoiding collapse.

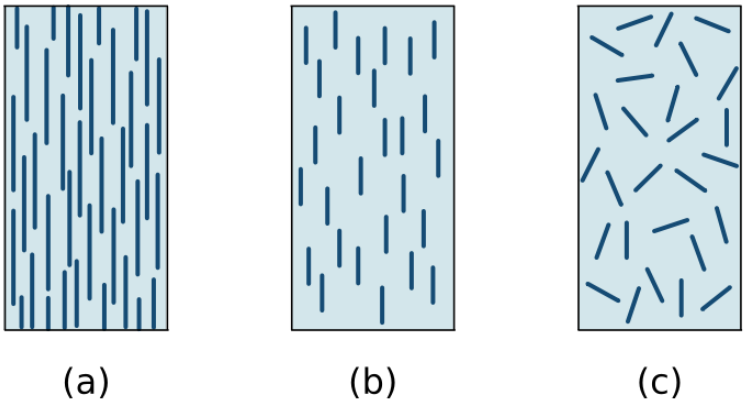

Fig. 4. Fiber reinforced composites types [4]

Fiber Reinforced Composites in turn represent a great variety of materials. Main actors in the field are carbon fiber and carbon fiber-reinforced polymeric composites, glass fiber-reinforced polymeric composites, poly urea, aramid and natural fiber reinforced polymer composites.

2.4 Natural fiber reinforced polymer composites. NFRPCs became the focus of recent investigations due to the constant increase in public opinion consciousness and new environmental regulations. We can define natural fibers as fibers that are not obtained synthetically or human made. Natural fibers can be produced both in renewable or non-renewable ways.

Fig. 5. Fiber reinforced composites in a Mercedes Benz class 11 [5]

Natural fiber has several advantages over synthetic fiber such as low weight, low cost, good relative mechanical properties and biodegradability. Due to the superior properties

of natural fiber over synthetic fibers, natural fiber reinforced polymer matrix is being considered for several applications. If high specific strength and stiffness are desired in a NFRC, it can be obtained by adding natural fiber to a thermoplastic or thermoset polymer. One of the greatest challenges in this aspect is the bonding between the polymer and the fibers mainly because of the different chemical structures of the materials to couple and the moisture sensitivity of natural fibers. In order to obtain a high quality bonding, natural fibers must receive specific treatments. The NFPCs use and application is growing almost exponentially in several industries such as the aerospace industry, sports and construction industry with a special focus on the automotive industry.

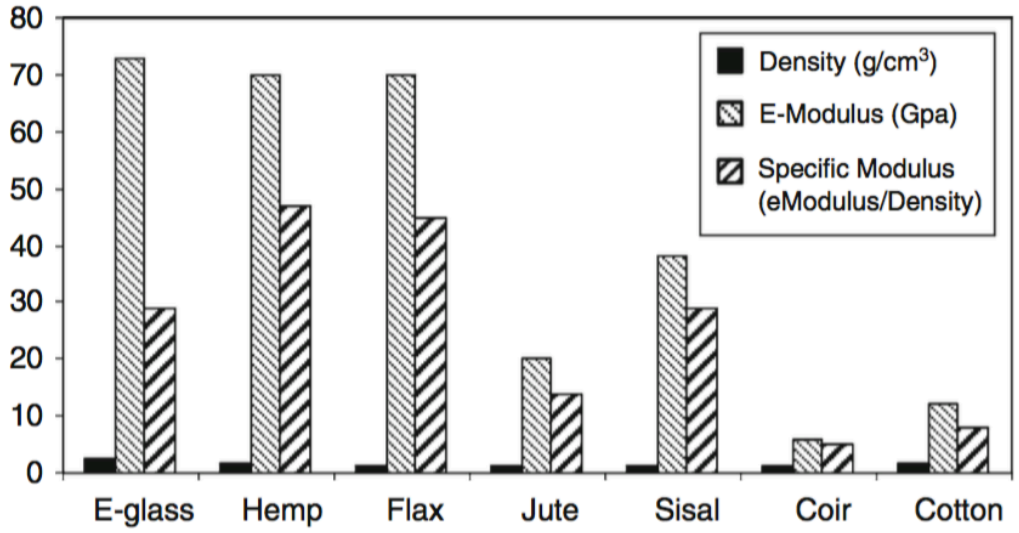

Fig. 6. Properties of some fibers used in NFRCs [Mohanty]

Natural fiber reinforced polymer composites (NFRCs) consist mainly of a matrix (polymer, thermoset or thermostat) and high strength natural fibers such as oil palm, jute, sisal…etc. The properties of NFPCs vary largely depending on what fiber and polymer are being used and the interface between both. The mechanical properties of NFRCs depends mainly on the orientation, strength, physical properties and interfacial adhesion property of fibers. Their mechanical efficiency is highly dependent on the interface provided by the fiber-matrix interaction, the hydrophilic behavior of fiber and the absorption of moisture must be reduced.

2.5 Natural Fibers – Structure and Properties. Natural fibers can be defined as mentioned above as fibers that are not obtained synthetically or human made and depending on their origin they can be classified into five categories: bast, leaf, seed, fruit and wood. Their chemical structure must be well understood for a rigorous decision to be made about the retrofitting material of the masonry wall.

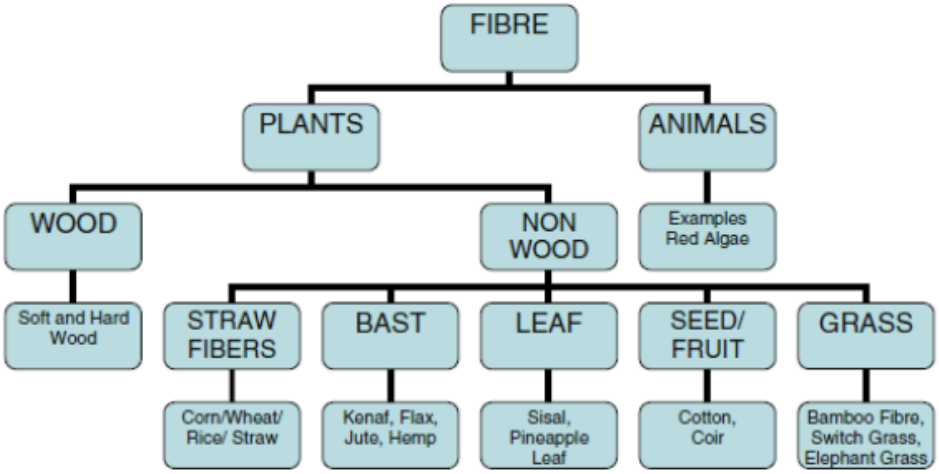

Fig. 7. Classification of natural fibers (Mohanty)

The three main components of natural fibers are: lignin, cellulose and hemicellulose which contain natural polymers and are found along the cell's wall. The last two, cellulose and hemicellulose belong to the family of polysaccharides. Cellulose is the main component of natural fiber and it is responsible for its strength and stability. It has a regular structure and is a highly crystalline polymer formed by many units of anhydroglucose with a degree of polymerization of around 10,000.

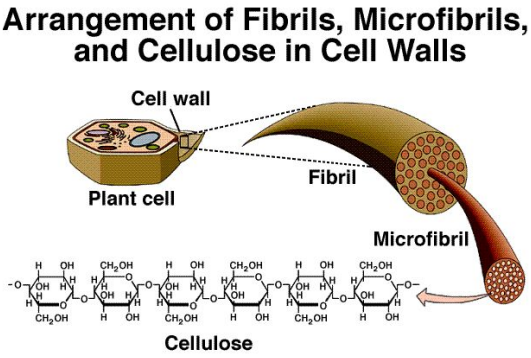

Fig. 8. Natural fiber structure and Cellulose [6]

Even though the molecular weight of hemicellulose is considerably inferior to the one of the cellulose, it still influences in the strength of the natural fiber. This polysaccharide is a shorter polymer formed by several carbon sugars (five to six carbons). The third component, lignin whose main function is to act like an adhesive with the cellulose fibers and keep the structure together consists of an amorphous polymer network, a disordered cluster of phenyl propane units.

Besides those main components, we can also find pectin, waxes and non-structural components with lower relevance. Those components even if not that relevant in the

structural properties of the material, play a key role when discussing about the bonding between the composite matrix and the fiber. Those extractives may change the surface of the natural fibers during drying and have a strong influence in the degree of adhesion to the matrix. The technique to eliminate extractives depends mainly on the type of extractives we are talking about. If the compounds are water soluble, then water treatment may fit, in other cases, treatments such as solvent extraction and steam distillation might be considered. Stem distillation is effective in removing compounds such as resin acids, fatty acids and alcohols or waxes.

2.6 Natural Fiber Reinforced Biodegradable Composites. The composites studied in this paper are Natural Fiber Reinforced Biodegradable Polymer Composites (NFRBPCs). Even if growing rapidly, the research in this area is still very limited compared to other areas such as thermoset or thermoplastic polymers mainly because of their scarcity and high costs. The development of natural fiber reinforced biodegradable composites suffered a smooth transition, first researchers in the field focused on the replacement of synthetic fibers in the composites with natural fibers maintaining the same matrixes. At that stage, and thanks to several countries involved the next step was obvious. Making the matrix itself bio-degradable and being able to obtain it from renewable sources instead of petroleum-based substances was the next milestone in the industry.

Fig. 9. Flax fiber composite fabric / woven [7]

As mentioned before, even today, research is focused mainly in the combination of natural fibers and petroleum based polymers and their mechanical properties rather than biopolymers. These combinations have many advantages, most of them already stated in previous sections in this paper, however they are not as environmentally friendly as biodegradable polymers. The combination between natural fibers and biodegradable polymers was the long-waited answer to a sustainable development in the near future.

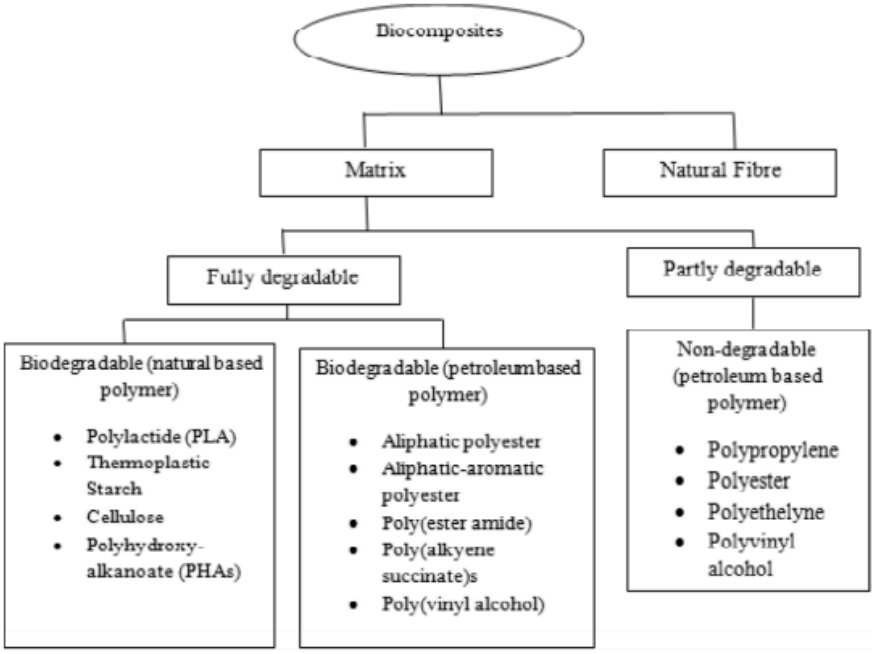

Fig. 10. Classification of biodegradable composites (also adapted from Mohanty)

These composites are the combination between natural fibers and a bio-resin. Bio-resins have several advantages respect to petroleum-based synthetic resin in terms of environmental friendliness. To mention some biodegradable resins: starch and starch blends, cellulose acetate, polycaprolactone(PCL), polyglycolide (PGA), polyhydroxyalkanoates (PHA), polilactic acid (PLA) and some other mixtures. Bio-polymers can be separated into four main groups: natural polymers such as cellulose, natural polymers such as cellulose, synthetic polymers synthetized from natural monomers such as polylactic acid (PLA) and polymers developed using microbial fermentation like polyhydroxybutyrate (PHB).

Several research studies have revealed that the combination between natural fibers and bio-degradable resins can have in some cases equal or better properties than the combination with their synthetic counterparts. Better flexural strength and elastic modulus respect to hemp/polypropylene using hemp/cellulose acetate composites [Ochi] , using emulsion type biodegradable resin and Manila hemp fibers has obtained a significantly high tensile and structural strength. Compared to hemp/polypropylene, the tensile strength and Young's modulus of the combination between unidirectional hemp fibers and cashew nut shell liquid is higher. If the hemp fiber is treated wish alkali treatment, the strength reaches even higher tensile strength values almost equal to values present in glass fiber/polyester composites.

Same behavior as in mixes of natural fibers and synthetic polymers, treatment to the fibers influences in a favorable manner the properties of the composites leading to a notable increase in tensile strength and Young's modulus values. As stated in previous sections, treatment focuses on improving the bonding between the fibers and the matrix, the so called interface of the composites. Better composites can be achieved using

several treatments such as alkali treatment, hot water treatment, heat treatment or salt water treatment. With the correct treatment applied, natural fiber biodegradable composites can reach similar properties to their synthetic counterparts.

2.7 Natural fibers / poly lactic acid (PLA). Compared to the research on thermostat and thermoset polymers, the research on biopolymers is limited. Poly (lactic acid) is a compostable synthetic polymer developed with a monomer derived from corn starch that can also be derived from rice, potato or any other agricultural waste. PLA is a good fit for applications where high performance is not needed. PLA synthesis is quite straightforward, first the raw material mentioned above is converted to dextrose witch afterwards undergoes a process of fermentation using a catalyst and converts into lactic acid. The monomer is afterwards purified and in a presence of another catalyst the polymer starts forming.

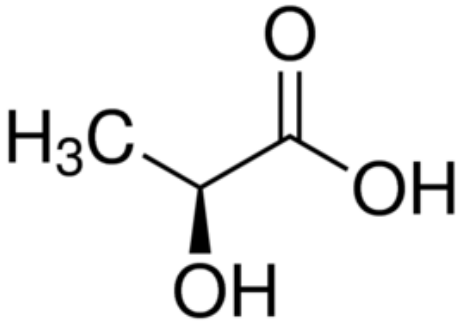

Fig. 10. Lactic acid

Due to the fact that its melting temperature is around 150º C to 175ºC, its processing can be done using traditional methods such as injection moulding, blow moulding, film operations and extrusion. Compared to petrochemical polymers, its mechanical properties are often times similar or superior which make PLA an interesting substitute for mass production polymers. One of the draws of PLA is its brittle nature which leads to a material with low toughness. One solution to that is the incorporation of natural filters in the polymer matrix. Filters are also used in polymer matrixes in order to increase the cost efficiency of the material, they have a high abundance and are low cost.

There are several factors that affect the eligibility of natural fibers used in PLA composites and their development such as thermal stability, moisture content, processability, fiber dispersion, fiber-matrix adhesion, surface modification of natural fibers and the fiber aspect ratio. In the experiments developed by Oksman, cellulose fibers have been used as a reinforcement for a PLA matrix. Using triacentin as a plasticizer which facilitates a better fiber dispersion in order to combat the brittle nature of PLA. Several other studies describe the developments reached by other researchers in terms of possible combinations of PLA with natural fibers such as flax, hemp, ramie, etc (Wollerdorfer).

2.8 Natural fibers / thermoplastic starch composites. Since the 1980 when bio-composites become the focus of serious developments and biodegradable matrixes reinforced with natural fibers gained more and more attention, starch has been one of the most used matrixes becoming the most popular solution for this kind of composites. In this section a review of the latest research studies using plasticize starch and natural fibers is exposed in order to situate the reader.

Taking advantage of the injection modeling process, jute strands and biodegradable starch have been used in order to develop a starch based composite. Afterwards the properties of several samples playing with the percentages of each component using alkali treated jute and untreated jute have been exposed. Detailed information about the findings and the process can be found in the biography. They proved that the strength increased proportionally with the percentage of fibers up to a 30% percentage of jute strands. Also, treated strands with alkali treatment seemed to increase the strength and also the resistance to moisture which from the beginning was high.

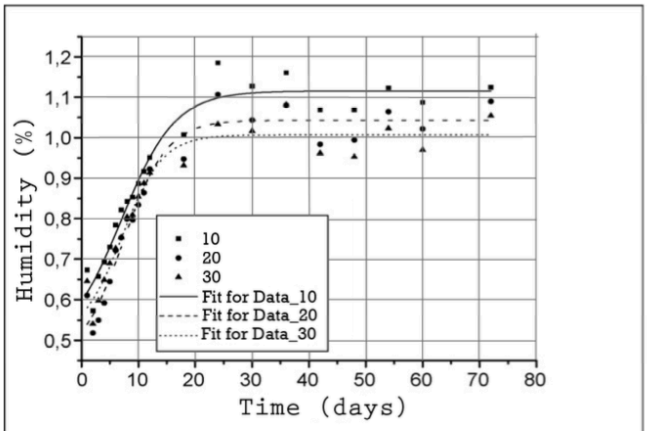

Reinforcement (%)	Initial (A_1)	Final (A_2)	X at Y=50 (X_0)	Width (dX)	Correlation (R^2)
10	0.47748	1.1155	7.0021	4.7151	0.9616
20	0.44191	1.0431	7.3101	3.8306	0.9574
30	0.50629	1.0068	7.1514	3.5046	0.9484

Fig. 11. Moisture absorption of untreated jute strand/starch in terms of Boltzmann parameter [9]

As a conclusion, the structural properties decrease with the increase in temperature and increase with the increase in fiber content up to a limit, this behavior is detailed in Fig. 5.

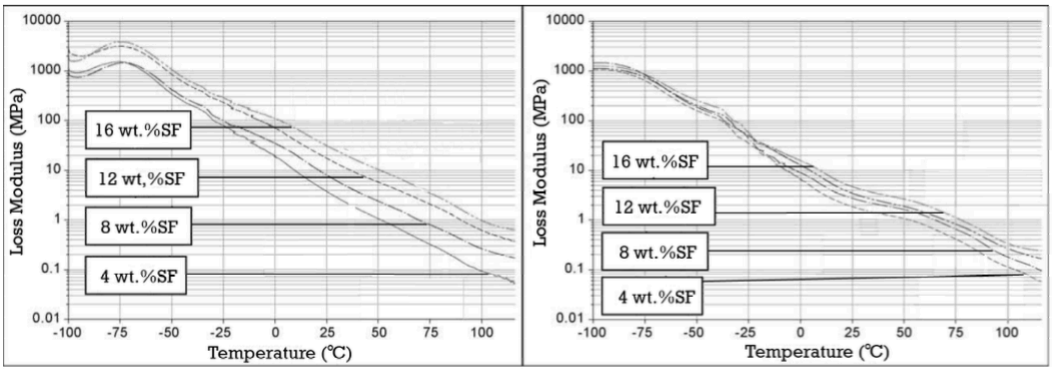

Fig. 12. Loss and storage modulus loss versus temperature increase [9]

Several experimental test have been made testing the relations between the length of the fibers versus the reinforcement effect. The general conclusion is that the reinforcement effect increases when increasing the fiber length from short to medium. However, studies present discrepancies when talking about elongation at break. Another study by Averous reveals that an increase in the main transition temperature leads to an increase in the mechanical properties. As a occlusion we can say that thermoplastic starch is a viable option to use with natural fibers and the properties of the composites obtained by those mixes are present good mechanical properties.

2.9 Natural fiber / cellulose composites. Cellulose derivatives have also been considered as a viable option acting as a bio-degradable matrix, however few studies have been performed in this area. A short review of the state-of-art of research of cellulose composites and their properties is presented in this section. Cellulose derivatives are a good fit for matrixes in biodegradable composite, techniques such as injection moulding, extrusion and rotation moulding. However, even if the fibers improve tensile and flexural properties, the impact strength of the composite is reduced.

2.10 Natural fiber / PHAs composites. Polyhydroxyalkanoates (PHAs) represent a category of biodegradable polyesters that are considered as viable substitutes to petroleum-based plastics. Those polyesters are synthetized via bacteria and a reviews of their possible composites with natural composites are presented in this section. With bamboo fiber and bacterial polyester, Singh and Mohanty developed bio-degradable composites using injection moulding techniques. Those bio-degradable composites have shown a steady increasing tensile modulus with the fiber loading. However, there was a decrease in tensile strength which was due to the lack of interaction between matrix and fibers. Reinforced composites show however an increase in tensile and flexural modulus of around 167%. It was also concluded that increasing the fiber loading can lead to an increase in the storage modulus.

3. Numerical model for Masonry Wall – Material model selection

As discussed in the introduction, a key element in the success of the approach exposed in this paper was the choice of the material model. In order to make an appropriate choice, several factors have been considered, therefore the material of the wall, the boundary conditions and the processes the wall will be exposed to have been taken into account carefully. During this process we must keep in mind at all time that we are dealing with an elastic-plastic material exposed to a high component of hydrostatic pressure with a high probability of failure.

Masonry consists of a composite material formed by bricks and mortar. Its behavior is not easy to predict, the main difficulties arising from the many possible failure modes, complex material models and the construction quality in real life models. In order to simulate the non-linear behavior of masonry walls and structures, historically researchers have taken three approaches, one known as macro-modeling, another known as simplified micro-modeling and other known as detailed micro-modeling, depending on the level of accuracy desired. A more detailed view on the existing strategies enumerated from less to more in terms of complexity:

- Macro-modeling: here masonry is considered a continuum material and the interface between the interface between both off its components is considered negligible.
- Simplified micro-modeling: the behavior of the mortar joints and brick-mortar interfaces are represented as discontinuous elements and the expanded units are represented by continuous elements.
- Detailed micro-modeling: bricks and mortar are represented by continuous elements and the interface between both by discontinuous elements.

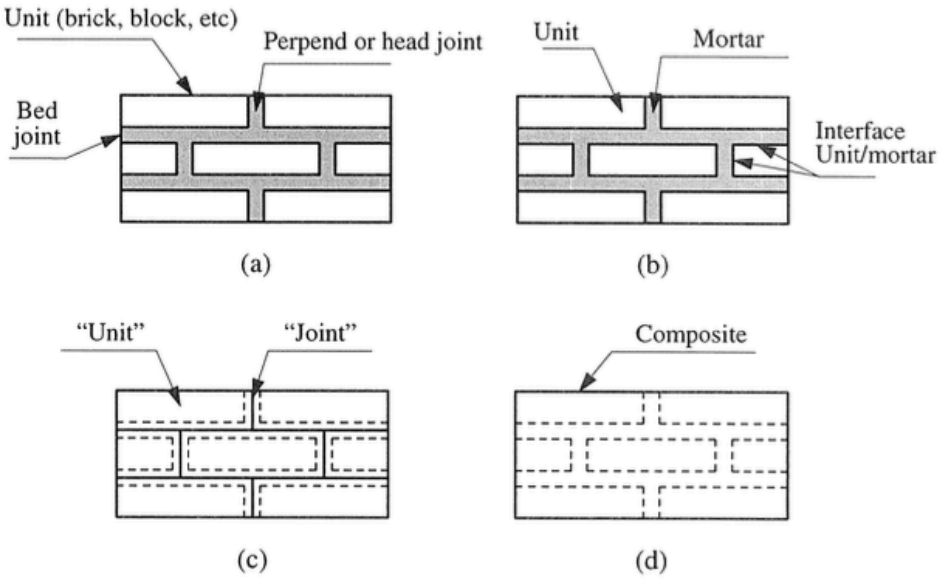

Fig. 13. Modeling techniques for masonry: a) masonry sample; b) detailed micro-modeling;
c) simplified micro-modeling; d) macro-modeling. (Laurenco in [2])

The macro-modeling technique simplifies the analysis because it makes no distinction between bricks, mortar and the interface between both. The material is modeled as a continuum anisotropic or orthotropic material and the average stresses relate with the average strains. This model is the simplest to use and understand and it is considerably faster than others. It requires less analysis and computational time as well.

3.1 Finite elements and plasticity. This paper adopts the finite elements method for simulating structural behavior. In order to make use of this model, a constitutive model is needed. Constitutive models represent a mathematical model for the material behavior which offer a relation between the stress and strain tensors. The constitutive models presented here will be formulated using a plasticity framework. This constitutive model represents a simplification of reality. Even if simplified, this model increases the possibility of the mesh to converge, matter which makes it more practical than more complex and detailed models that run the risk of failure to converge. Our challenge is using the model that is able to effectively predict the material behavior from the elastic phase all the way through the cracking until reaching failure.

The theory of plasticity will be used as a framework for our model. This theory has well established models especially for metals (Hill 1950) but it can be easily applied to quasi brittle materials as well. This section will introduce the finite elements solution and some basic aspects of the theory of plasticity. For more details, the reader can look into Hill (1950) and Chen and Han (1988).

3.2 Nonlinear finite elements. Finite elements methods are based on the displacement method, the structure is divided into small elements, each of them having its own material properties and relationships between nodal forces and displacements. All those elements are afterwards assembled considering external loads and boundary conditions. This results into a system of equations that describes the equilibrium of the structure which will be solved and give as a result the nodal displacements of the structure. The displacements can be numerically integrated later on in order to obtain stress and strains at each element.

In this section we will illustrate two element types widely used in masonry, one for the unit stress and the other one for the interface between units. In the case of the unit a plane stress continuum element is used. The constitutive model for this element defines the relation between the stress and strain tensors using the stress vector and the strain vector as:

$$\sigma = \{ \sigma_x \, \sigma_y \, \sigma_z \}^T, (1)$$

and

$$\varepsilon = \{ \varepsilon_x \, \varepsilon_y \, \varepsilon_z \}^T, (2)$$

In the case of interface elements, discontinuities are allowed in the displacement field and a direct relation between the traction denoted as t and the relative displacements denoted as deltau is established:

$$t = \{ \ \sigma \ \tau \ \}^T, (3)$$

$$\sigma = \{ \ \Delta u_n \, \Delta u_s \ \}^T, (4)$$

The zero-thickness interface can be obtained by degenerating the continuum element, Hohberg (1992). This will allow us to define generalized stress and strain vectors and use a standard formulation which is really attractive because of the simplicity it adds to nomenclature.

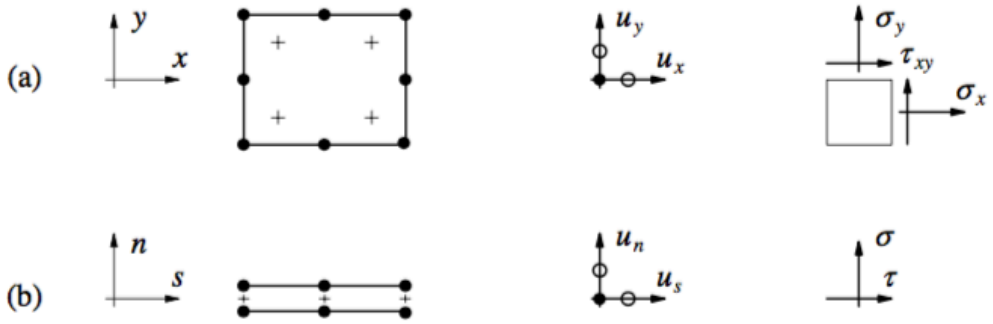

Fig. 14. Finite element utilized in this paper. (adapted from Laurenco 1996 [2])

As next steps after formulating the model, one of the key factors in the success of our solution will be selecting the right integration scheme. According to Rots (1988) and Schellekens (1992), the Gaus scheme may lead to erroneous results in stress oscillations. Following Laurenco, the scheme illustrated in this paper as an example is the Lobatto scheme.

3.3 Iterative techniques for solving non-linear problems. The non-linearity of those problem is mainly due to the inelastic constitutive laws exhibited by materials property and the complex dependency of the stress vectors on its strain counterpart. In order to fulfill equilibrium and the appropriate constitutive laws, a solution is needed which will adjust the material parameters. This solution will be found iteratively by trial and error. We must keep in mind that the solution to non-linear problems does not necessary exists

and if it does, it doesn't have to be unique. This leads to a converged solution, a realistic one that is usually obtained using incremental approaches where the load is separated in small steps.

In the example of discretization of the problem, the scheme provided by Laurenco (1996) has been used. The reader must keep in mind that this demonstration serves as an example and tries to provide an understanding of what later on will be simulated as mentioned in previous sections using ABAQUS. In this case, the software will do the simulations and sole the convergence problem using its own solving schemes. However, as future engineers using the software we must have a basic understanding of the computations in order to provide an accurate interpretation of the results the iterations done by the software.

Following Laurenco, we can discretize the problem using a vector that collects all the nodal displacements, a. The system of equations at the step n+1 looks like:

$$\Psi_{n+1} = \Psi(a_{n+1}) = p(a_{n+1}) - f_{n+1} = 0 \quad (5)$$

Here Ψ represent the vector of unbalanced forces, with p being the vector of internal forces and f being the vector of external forces (equilibrium equation). The equation from the previous stage, n represents equilibrium:

$$a = a_n, \qquad \Psi_n = 0, \qquad f = f_n, \qquad (6)$$

and changes when the next incremental step in the load is applied with,

$$f_{n+1} = f_n + \Delta f_{n+1}, \qquad (7)$$

With the purpose of determining the change in displacements vector, Δa_{n+1}, such that,

$$a_{n+1} = a_n + \Delta a_{n+1} \qquad (8)$$

the load increment will be small avoiding falling out of the radius of convergence. Other researchers have proposed self-adapting loading schemes, but illustrating them falls out of the purpose of this paper.

The problem is now solved in Laurenco using a locally quadratic convergent Newton – Raphson method similar to the ones studied in the bachelor. The method is derived by finding the root of an approximation of equilibrium equation at the current state using second partial derivative equations:

$$\Psi(a_{n+1}^{i+1}) = \Psi\left(a_{n+1}^{i}\right) + \left(\frac{\partial \Psi}{\partial a}\right)_{n+1}^{i} \delta a_{n+1}^{i+1} = 0, \qquad (9)$$

Using i to count the iteration steps and starting with $a_{n+a}^{0} = a_n$ and,

$$\left(\frac{\partial \Psi}{\partial a}\right)_{n+1}^{i} = \left(\frac{\partial p}{\partial a}\right)_{n+1}^{i} = (K_t)_{n+1}^{i} \qquad (10)$$

Where K_t is the tangential stiffness matrix. By replacing in equation … we get the iterative correction of the nodal displacement:

$$\delta a_{n+1}^{i+1} = -(K_t^{-1})_{n+1}^{i} \Psi_{n+1}^{i}, \qquad (11)$$

After successive approximations,

$$a_{n+1}^{i+1} = a_n + \Delta a_{n+1}^{i+1} = a_n^i + \delta a_{n+1}^{i+1}, \qquad (12)$$

with,

$$\Delta a_{n+1}^{i+1} = \sum_{k=1}^{i+1} \delta a_{n+1}^{i+1} \qquad (13)$$

until the convergence is obtained with the tolerance desired. As Laurenco mentions, one of the flaws of the Newton-Raphson scheme is that is not globally convergent, the method does not converge to some solution of the system nonlinear equations from almost every starting point.

A widely used solution for this matter in structural problems when proceeding form, a point outside of the radius of convergence of the Newton-Raphson method is the line search. Searching the direction is the most crucial step of this process, a detailed overview is present in Dennis and Schnabel (1983) and further on in Laurenco [2]. For structural problems, the technique consists of writing:

$$a_{n+1}^{i+1,j} = a_{n+1}^{i} + \mu_{ij} a_{n+1}^{i+1} \qquad (14)$$

where j is the iterative counter of the line searching and μ is the line search factor that scales the incremental displacement field. In order to determine the line search factor we must equal the projection of the residuals in the search direction δa_{n+1}^{i+1} to 0,

$$\left(\delta a_{n+1}^{i+1}\right)^T \Psi\left(a_{n+1}^{i} + \mu_{ij} \delta a_{n+1}^{i+1}\right) = 0 \qquad (15)$$

solved by using the secant equation. Generally, the additional energy cost of calculating the line search algorithm is negligible compared with the calculation of the internal force vector. However, there is a better performing condition than the one stated in previous equation 15 as stated by Dennis and Schnabel (1983). A commonly used criteria is:

$$\left|\left(\delta a_{n+1}^{i+1}\right)^T \Psi(a_{n+1}^{i} + \mu_{ij} \delta a_{n+1}^{i+1})\right| \leq \eta \left|\left(\delta a_{n+1}^{i+1}\right)^T \Psi(a_{n+1}^{i})\right| \qquad (16)$$

where η is a tolerance factor that for the Newton-Raphson method in most cases, equal to 0.8. It should be mentioned that if the step increments in the load are small and the problem is well formulated, the criterion is fulfilled from the first moment and no more line searches are needed.

3.4 Newton-Raphson method for softening behavior. As stated previously, in order for the schemes to work smoothly, the incremental steps in loading should be small and the must be some kind of load control. The easiest way to control the load in nonlinear finite element analysis is to use a load factor, $\Delta\lambda$. This is made under the assumption that the loads are proportional to an initial load vector, f_0:

$$\Delta f_{n+1} = \Delta\lambda_{n+1} f_0, \quad (17)$$

This standard control fails however at the points where equilibrium is reached and the next loading has a negative increment. In order to fix that, one can play with the displacement control and modify some degree of freedom. However further operations will show that only few engineering problems can be modeled this way and the technique is not able to deal with strong localizations. In order to fix those disadvantages, the arc-length method has been introduced and an extra constraint equation has been added to the original system which is rewritten as:

$$\Psi_{n+1} = p(a_n + \Delta a_{n+1}) - (\lambda_n + \lambda_{n+1}) f_0 = 0 \qquad (18)$$

$$f(\Delta\lambda_{n+1}, \Delta a_{n+1}) = 0 \qquad (19)$$

However, the system has been improved later on by Crisfield (1981) and Ramm (1981), also see Laurenco [2]. The nodal displacement increment can be written for a given iteration as:

$$\begin{aligned} \delta a_{n+1}^{i+1} &= -(K_t^{-1})_{n+1}^{i} \Psi_{n+1}^{i} \\ &= -(K_t^{-1})_{n+1}^{i} (p_{n+1}^{i} - f_n - \Delta\lambda_{n+1}^{i+1} f_0) \\ &= \{(K_t^{-1})_{n+1}^{i} (f_n - p_{n+1}^{i})\} + \\ \Delta\lambda_{n+1}^{i+1} &\{(K_t^{-1})_{n+1}^{i} f_0\} \\ &= \delta^I a_{n+1}^{i+1} + \Delta\lambda_{n+1}^{i+1} \delta^{II} a_{n+1}^{i+1}, \end{aligned} \qquad (20)$$

Here, $\delta^I a_{n+1}^{i+1}$ is found by subtracting the internal forces after the iteration step i to the external forces ate the beginning at the load step. $\delta^{II} a_{n+1}^{i+1}$ represents the external load component of the actual loading step. By replacing , $\delta^I a_{n+1}^{i+1}$ and $\delta^{II} a_{n+1}^{i+1}$ in the constraint equation we will be able to find $+\Delta\lambda_{n+1}^{i+1}$. Using the orthogonality of the tangent vector and the change in displacement vector after each iteration in the normal plane:

$$(\Delta a_{n+1}^{i})^T \delta a_{n+1}^{i+1} = 0 \qquad (21)$$

By substituting this in the previous equation we will get:

$$\Delta\lambda_{n+1}^{i+1} = -\frac{(\Delta a_{n+1}^{i})^T \delta^I a_{n+1}^{i+1}}{(\Delta a_{n+1}^{i})^T \delta^{II} a_{n+1}^{i+1}} \qquad (22)$$

However, this method has also been known to fail specially when dealing with strong localizations, De Borst (1986) proposed to restrict the number of degrees of freedom in the constraint equation. This solution has been reported as highly effective in the case of concrete cracks and cracks in composite laminates. In the case of cracking a good selection are the displacements on both sides of the crack. For further progress we should subtract those displacements which will lead to a mode I or mode II Crack Opening Displacement (COD).

$$\Delta\lambda_{n+1}^{i+1} = -\frac{\delta^I COD_{n+1}^{i+1}}{\delta^{II} COD_{n+1}^{i+1}} \qquad (23)$$

This strategy goes long in detail and it is mainly used for micro-modeling in masonry structures. As a summary we can state that an incremental-iterative Newton-Raphson method has been used to solve the system of nonlinear equations obtained using the finite element discretization. The Newton – Raphson method has been constrained using a normal plane method in order to avoid limit point or strong localizations. In order not to fall out of the convergence radius, the method has been improved using a line searching algorithm using a convergence tolerance of $\eta = 0.8$ and a maximum number of line searches of five.

In order to define the material behavior, we need a stress to strain relationship at any point of the body. A general formulation for all the modes of the composite yield surface is obtained using the theory of multisurface plasticity. The simulations present in this paper are however obtained using computational methods.

3.5 Materials under dynamic loading. When exposed to certain rates of loading and prior to failure and fracture events, structural materials can exhibit a rapid process so called hardening of softening phenomena. This material behavior adds more complexity to the already existing mathematical and numerical models. The mathematical model for the equations must be formulated with care. Lack of knowledge can lead to changes in equations that may lead to pathological mesh dependency. This change in equations can lead to meaningless results.

In order to avoid this type of changes, a procedure called regularization is implemented. The main motivations of the regularization process are the high order media for soil mechanics and the level of numerical discretization. For static problems, the equations should be elliptic as opposed to dynamic ones where the system should be hyperbolic. Explosions represent fast dynamic loading processes with high orders of deformation (between 10^3 and 10^6 s-1). A table providing load qualifications is provided below:

Load classification	$\frac{\tau}{T}$	Type of the load
Quasi-static	>4	Conventional testing
Quasi-static	1	Transient loading on structures
Impact	<0.25	Kinetic energy, blasts pressure
Shock	$<10^{-6}$	High energy explosives

Fig. 15. Load types [2]

3.6 Softening behavior of masonry structures. A noticeable characteristic of quasi-brittle materials like bricks, mortar, rocks or concrete which represents a slowly progressing decrease of mechanical properties when the structure is exposed to a continuous increase in deformation. This behavior is due to the heterogeneity of the material, the presence of so many different phases and material defects. In practice, this structures already contain micro-cracks and inclusions due to the manufacturing process even before loading. Those initial defects, internal stress concentrations and micro-cracks and variations in the internal stiffness and properties cause progressive crack growth when the material is subjected to continuous deformation. At the beginning, this behavior is stable because the micro-cracks growth depends directly on the load applied and whether is applied or not, they grow only if the load is applied. However, when a peak load is reached the behavior becomes unstable, the crack formation accelerates and becomes unstable and macro-cracks start to appear leading to an uncontrollable growth if the loads keeps applying.

This behavior has been well studied in the case of tensile failure. For shear failure, this process has also been observed. However, in the case of compressive failure, this process is highly dependent on the boundary conditions and the size of the experiment. The characteristic stress-displacements diagrams are shown below in Fig. 5 for quasi-brittle materials. In the study (Lourenco 1996 – 2013) one of the assumptions is that the inelastic behavior both in tension and compression can be effectively described by the integral of the stress/displacement curve. The results of these integrals are the corresponding fracture energies for both tension and compression denoted as G_c and$G_f$and are assumed to be material properties.

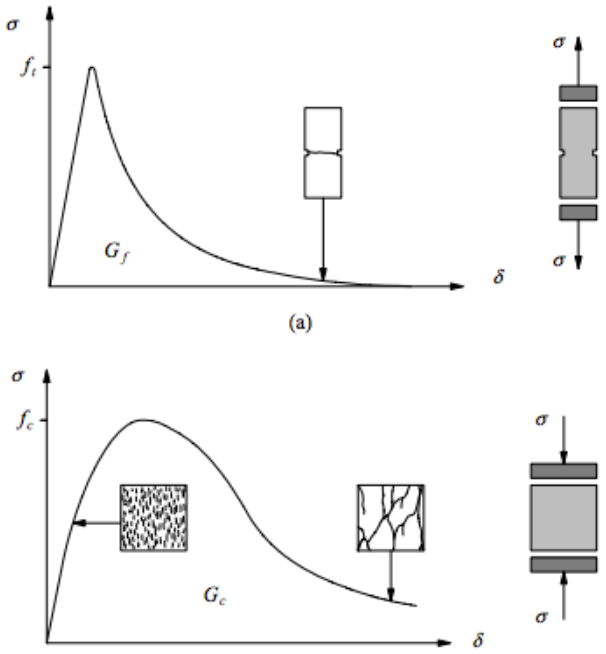

Fig. 16. Behavior of quassi-brittle materials under loading (uniaxial) [2]

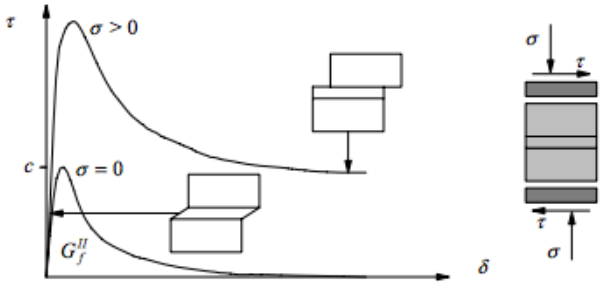

Fig. 17. Behavior of masonry under shear [2]

Because the failure mechanisms are identical (micro-crack growth), the approach on softening can be described with this energy-based thesis. However, we must account that masonry presents other failure modes, for example the slip of the brick-mortar interface under shear stress generally known as Mode II. Shear failure is a common cause of failure in masonry structures which must be accounted for, especially in micro-modelling strategies. However, when micro-modeling, this failure mode cannot be included because the geometry of bricks and mortar is not discretized. In those models failure will be mainly related with tension and compression.

3.7 Properties of brick and mortar. Masonry properties, as in most composites depend strongly on the properties of its components. One can use the compressive strength of the components in order to determine the strength of masonry, this process gives a good approximation; however, a true and accurate value of those properties is not easy to obtain. Using techniques of homogenization, several methods have been historically used to approximate the homogeneous masonry material properties. Most tests refer to

cubic specimens and cannot account for true strength. In the case of masonry, it is not easy to relate the tensile strength of the structure with its compressive strength due to the different materials, shapes and manufacturing processes. The properties used in this paper have been extracted from Laurenco 1996 and are shown in the figure below:

Parameter	Value
Elastic properties:	
- Density (kg/m^3)	2000
- Modulus elasticity (N/m^2)	16700
- Poisson ratio	0.15
Inelastic properties:	
- angle of friction (β)	46°
- flow stress ratio (K)	0.8
- dilatation angle (□)	20°

Fig. 18. Material properties for brick and mortar [7]

As a conclusion to this section, we can say that masonry can be considered as a composite material that consists of clay bricks and mortar. The failure mechanisms present in both tensile failure and compressive failure are essentially the same due to the micro-crack growth that evolves into an unstable macro-crack growth. In this process fracture energy is released from internal fractures and we have inelastic strain as a result. Masonry however can show another failure mode, identified as mode II due to shear failure after the softening has been completed.

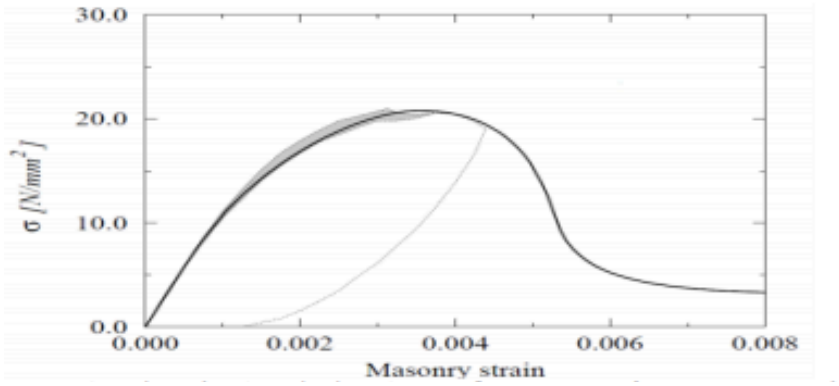

Fig. 19. Compression hardening for masonry [7]

If the approach to our experiment consists of micro-modeling, all these phenomena must be taken account of. However, in a macro-modeling strategy all those phenomena incorporate themselves under the anisotropic homogeneous continuum and the effects of interaction between bricks units and mortar will be considered negligible, establishing a relation between average stresses and strains instead. Leaving aside our choice of the type of strategy, in order to obtain accurate results, a complete description of material properties must be available. As seen previously this is not always the case due to the difficulties encountered in the manufacturing processes and testing. Experimental data is not easily available, this is why this section has reviewed masonry

properties and provided a table of properties to be used as guidance for further simulations.

3.8 Micro-modeling strategies. Micro-modeling techniques are more complex and focus on the individual properties and arrangement of bricks, mortar and the interface between them. This approach requires an exhaustive analysis coupled with several experimental tests calibrating material parameters. The technique requires a large number of elements for finite elements models even for relatively small structures, however they lead to a better understanding of the behavior of masonry at a local level. In those models, the bricks and the mortar are represented by continuum elements as opposed to the interface between both that is represented by discontinuous elements.

The structural properties (Poisson's ratio, Young's modulus, inelastic properties ...etc.) of both brick and mortar are taken into consideration and the interface between both which represents a potential crack/slip plane is studied in detail.

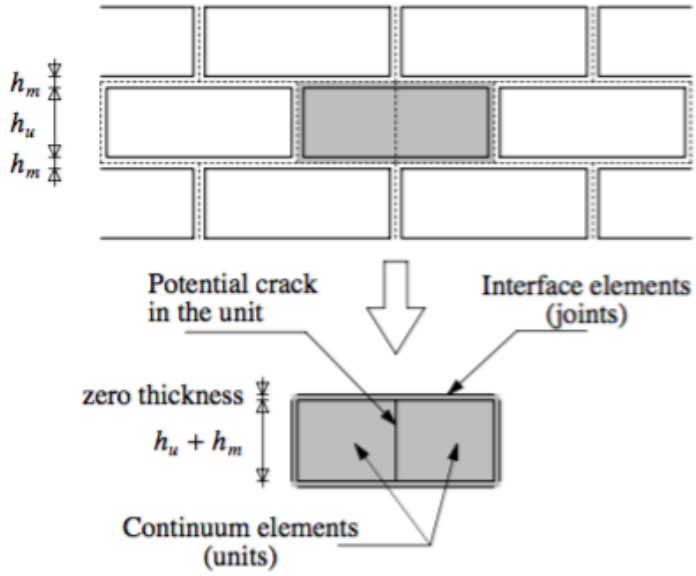

Fig. 20. Micro-modeling recommended strategy [2].

The micro-modeling approach is best fit for small structures with a special focus on the states of stress and strain. Its objective as already mentioned is to closely analyze masonry and the properties of each of its components. The material data must be collected experimentally in the laboratory from masonry samples and individual samples of mortar and bricks. However, those kind of models require large experimental and computational times that are not fit for the context of this paper.

3.9 Macro-modeling: An anisotropic continuum model. In real life our model must be first of all practical, the interaction at interface between bricks and mortar will be considered as negligible. In this macro-modeling approach, no difference is made between individual units and joints and the material is considered as an anisotropic composite with a relation between average strains and average stresses. Several macro-

models have been taken as references. The research in this area is poor and few macro models are available due probably to the difficulty in modeling the inelastic behavior of masonry. The approach taken in this paper is a macro-modeling technique, using ABAQUS and considering masonry as continuum material with constant properties and no imperfections. This will reduce computational time and needs and will give us a more mesh friendly model. This technique is also referred as homogenization which we can define as a process of averaging material properties and separating the composite properties from the properties of its components.

The analysis of big masonry structures can be realized making use of macro-models where, as mentioned above a relation between average stresses and average strains. Even if the constitutive behavior of the components of masonry, brick and mortar is isotropic, due to its geometrical arrangement, the behavior of masonry is anisotropic. We will be able to model masonry as a composite with numerical implementations of anisotropic plasticity. It should be noticed that many models in this field have only been proposed theoretically and not many numerical implementations are available.

3.10 Anisotropic continuum model. In order to effectively analyze the behavior of masonry structures, a macro-modeling analysis should count with a material description for all stress states. However, in the case of masonry, as stated in previous sections very few reliable experimental data are found and the complexity of formulating anisotropic inelastic behavior is just another block in the road. Laurenco used modern plasticity theory and a representation of anisotropic material behavior including hardening and softening behavior in order to develop a yield surface for masonry.

As stated there are basically two approaches when macro-modeling masonry. On the first hand, the material behavior can be described using only one yield criterion. Several attempts have been made using Hoffman yield criterion but the results were not a good fit for the experimental data obtained for masonry. Literature holds example of other failed attempts using Hoffman yield criterion, however it has been proved that this method is not accurate. The second approach extends isotropic quasi-brittle behavior formulations. This strategy has been employed by Fenestra and De Borst, who coupled the use of a Rankine and a Drucker-Prager criterion in order to analyze concrete behavior. Laurenco coupled a Rankin type criterion for tension and a Hill type criterion for compression.

3.11 Failure criterion. After taking a look at the existing strength criterions that might fit to our simulation and the purpose of this paper, and the historical approaches taken by other researchers several models come to mind. However, the strength criteria employed must fit the macro-modeling strategy we used approaching the problem. A short overview of the different strength criterions and material models considered is shown below:

Von Misses model – the simplest yield criterion that treats yielding as a purely shear deformation process and considers that it begins when the second deviator stress invariant (also formulated as yield strength) reaches a critical value. This model's simplicity makes up for its greatest strength and greatest weakness at the same time.

The model relates the tensile yield stress, shear yield stress and compressive yield stress through simple equations and it best applies to ductile materials. Prior to the yield, the material is considered elastic. During the blast impact on masonry walls, besides the shear component, the hydrostatic component has a huge impact in the yielding, component that is not accounted for in the Von Misses Criterion. This factor made the model ineligible for our simulation.

Linear Drucker-Prager model – this model has been formulated by Drucker and Prager in 1952. This criterion describes pretty well pressure-sensitive materials like soil, rock, concrete and masonry (masonry exhibits a pressure dependent yield, it becomes stronger as the pressure increases). The criterion is obtained slightly modifying the Von Misses criterion by introducing a parameter (μ) that accounts for the sensibility of yielding to hydrostatic stress. The hydrostatic stress sensitivity parameter is determined using two different stress states, tension and shear. However, the Linear Drucker-Prager models is not accurate for describing non-linear behavior of materials. To obtain the Drucker Prager model we modify the Von Misses criterion and introducing the hydrostatic sensitivity parameter:

$$\sigma_e = \sigma_o - \mu\sigma_m, \qquad (24)$$

Where the σ_o is a material parameter related with the shear yield stress by:

$$\sigma_o = \sqrt{3}\sigma_s, \quad (25)$$

And σ_m is the hydrostatic stress as a function of the principal stresses:

$$\sigma_m = \frac{1}{3}(\sigma_1 + \sigma_2 + \sigma_3) \qquad (26)$$

Equation (1) is the one that ABAQUS uses for its Drucker-Prager model in the finite element model where the nomenclature used is:

$$q = d + ptan(\beta), \quad (27)$$

with q = σ_e, p = $-\sigma_m$, tan(β) = μ and d = σ_o. For further information refer to[3].

4. Implementation of the model using ABAQUS for an unprotected Masonry Wall under explosion using a simple elastic material model

4.1 Modeling the masonry wall in ABAQUS:

First of all, we create a new file. For the sake of simplicity, we will call it wall. Our modeling space will be 3 – dimensional and the type of model will be deformable. For the type of the part, we will choose Solid and the part will also be created using an Extrusion. In order to determine the approximate size, we use the value of 20 which was determined using the real dimensions for the wall to be analyzed.

Now ABAQUS will bring up the 2-D sketching view port. Now from the tools panel we will select the create rectangle tool that we will use to draw the profile of our masonry wall. First of all, we will create a simple rectangle. As a next step we have to insert the dimensions we wish for our rectangle. For this we use the dimensioning tool, for the height we will use 3 meters and for the width we will use 5 meters. After the sizing process, the sketch has been finished and we can proceed with the extrusion and creation of the desired wall. ABAQUS will ask for the depth of the extrusion which has to correspond to the standard depth of a brick wall, in this simulation the standard depth of the brick wall used has been 0,215 meters.

As a result, our 3-D wall has been created. As a next step we will have to create a material to apply to the wall. We double-click on materials, and we call this new material Masonry. In order to define this new material, we will have to specify a few characteristics such as mass density: 2000 kg/m3 for masonry, the young modulus: 118e8, Poisson's ratio: 0.15. Now that the material has been created we have to assign it to the wall, we will do that by creating a section, using solid and homogeneous and properties. Now we will assign the newly created material called Masonry to the new section created and assign this new section to the wall.

After the material has been applied, the next step is to assemble the module. We open up the Assembly, double-click on instances, and leave about everything as it is. As it is only one part it doesn't matter if we choose dependent or independent but we will leave it as independent, so the mesh will be on the instance. Once this is done we have to create the analysis steps.

4.2 Creating the Analysis Steps:

The purpose of the analysis steps is to indicate ABAQUS what do we want to model. In this case we are modeling a blast explosion. We are going to create the blast explosion by double clicking on steps and creating a new step. For the sake of simplicity, we will call it Blast and we will also choose Dynamic Explicit for the procedure type because that's the best to describe a blast explosion. On the time period we will chose 0.01 which is the time period corresponding to a normal blast explosion.

Next step now is to create the boundary conditions to the wall. Again, for the sake of simplicity we will call them fixed. We will make sure to select initial, so that the boundary conditions are applied from start to finish, we will also choose Symetry, Antysimetry, Encastre. By selecting the four edges of the wall, we apply the desired boundary conditions, now all the edges will be fixed. Now press ok and select ENCASTRE, all the edges are completely fixed.

The next step now is to apply the loads. The load will be called Blast Load and will be assigned to the Blast. For the type of load, we will choose pressure, because is the one that best describes the blast load. Now we select the face of the wall we want the pressure to be applied. The distribution will be uniform and the magnitude will be set to 1. In order to simulate the blast in the most accurate way possible we will create a tabular amplitude, which means we can apply a linear force to the wall within the time period. It means that at the time period 0 we will apply a load with an amplitude of 1021250 Pascals and after 0.01 seconds it will go down to 0. So load has been now applied to the wall.

As a final step, we need to create a mesh. The family of the mesh is 3d Stress and the element library is Acoustic. The next step is to seed an instance. Now is time to set an essential parameter for the mesh, the approximate global size. In order to obtain the maximum efficiency for the mesh the smaller the size the better, that would give us a better accuracy, however it would also increase the computational time. However, the ABAQUS edition used in this paper is the Student edition, which is limited up to 1000 nodes. Now in order to find the best mesh size for our wall that will also have less than 1000 nodes we have to do a mesh convergence test.

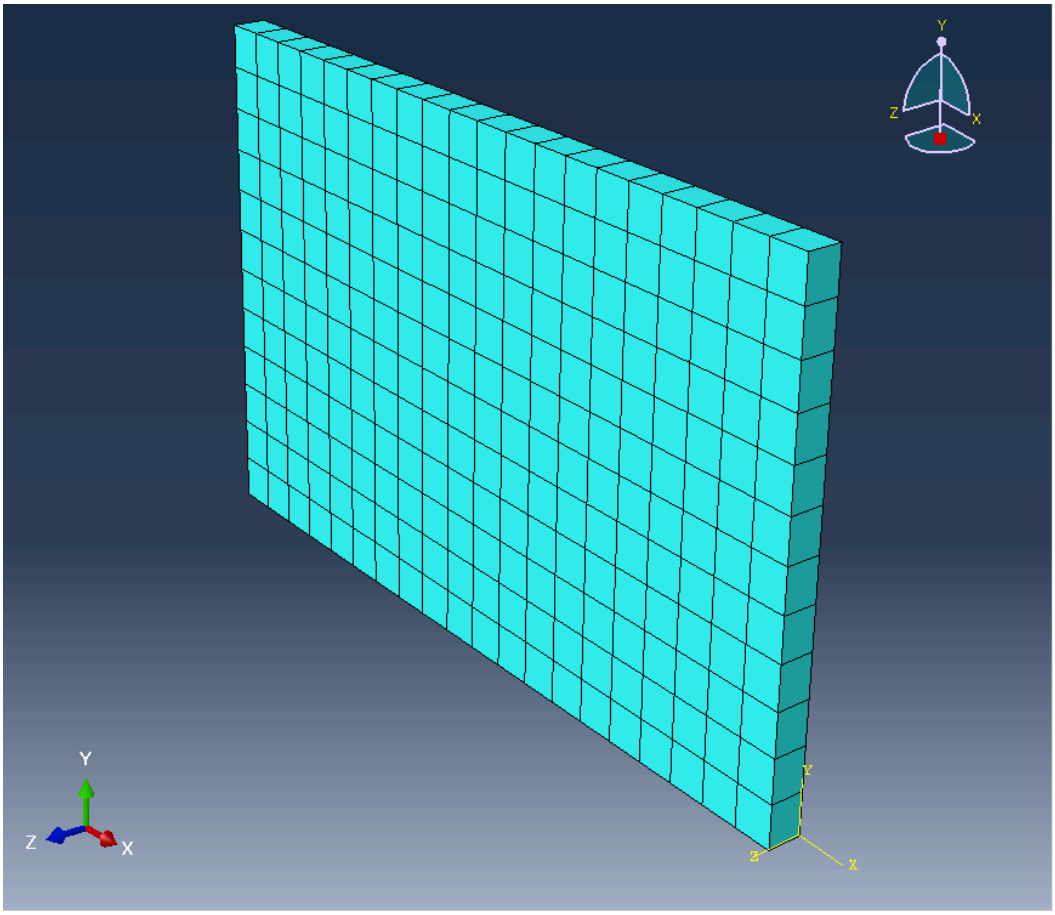

Fig. 21. Meshed masonry wall

After the test, the approximate global size found that best fits our constrains was: 0.1. Now the model has been meshed. As a final step we will have to submit the job for analysis. Now ABAQUS will analyze the wall. After the computations are over we can proceed to the final stage of the process, the Analysis Phase.

4.3 Analysis of the Results:

The job has been successfully completed. After the computations are over, we can access the results tab where the response of the wall under the blast explosion can be analyzed in detail. Now we right click on the job and scroll down to Results. If we click on Results, a visualization window appears. First of all, we are going to look at the displacements (Primary – U). We can display the evolution of the displacements during the blast explosion.

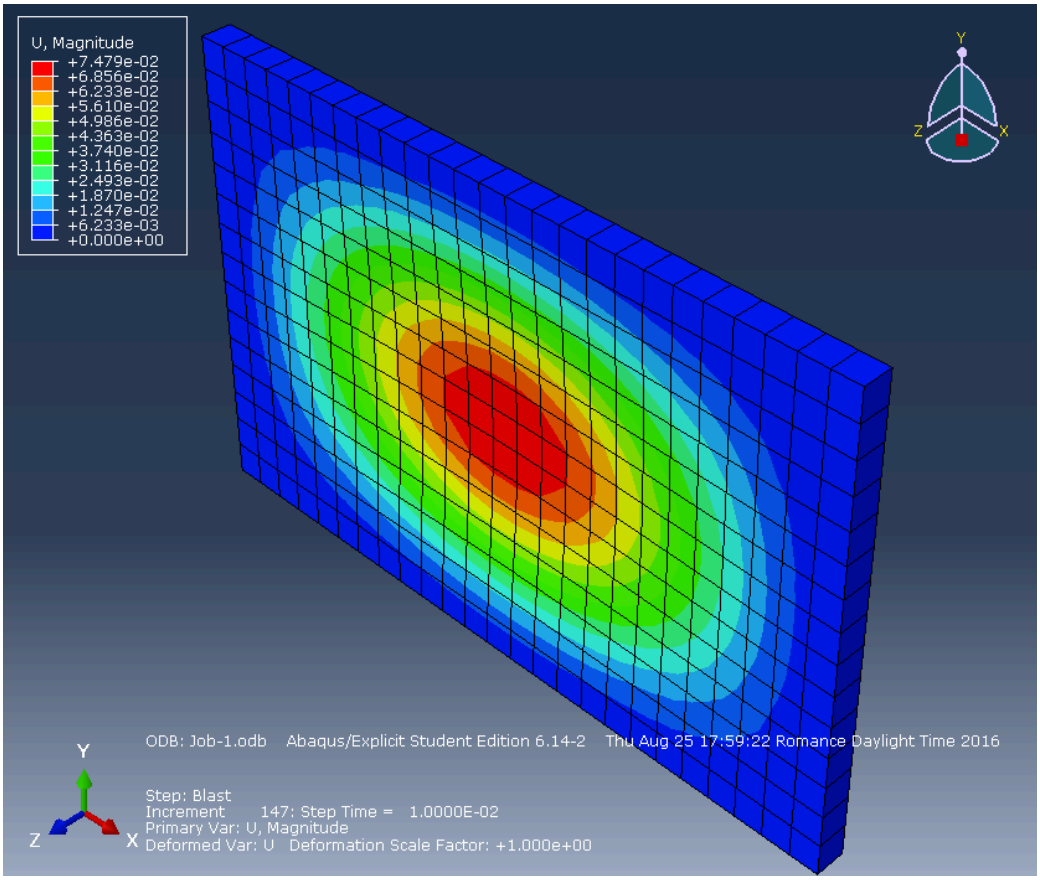

Fig. 22. Wall displacement for an elastic model

As we proceed further on, the displacement tends to focus on the center of the wall and we get a displacement on the center of the wall of around 7,59 centimeters. As we can see, the main displacements are in the center of the wall.

We can have a more in-depth look to this displacement by going to Tools, selecting the XY data tab and click to create. We use the ODB field output source and we are going to look to a particular node in the center of the wall. We select the Unique Nodal and chose the output variables we want to plot in the XY chart, in our case we select the sub option Magnitude in the Spatial Displacement tab. Afterwards going to the Elements/Node tab, we select a method and create a new section. We click Add Selection and select the node in the center of the node. Afterwards we click on Plot and a graph appears. As we can see, ABAQUS plotted the displacement of the node versus time of the explosion. The graph illustrates very well the elastic behavior of the wall:

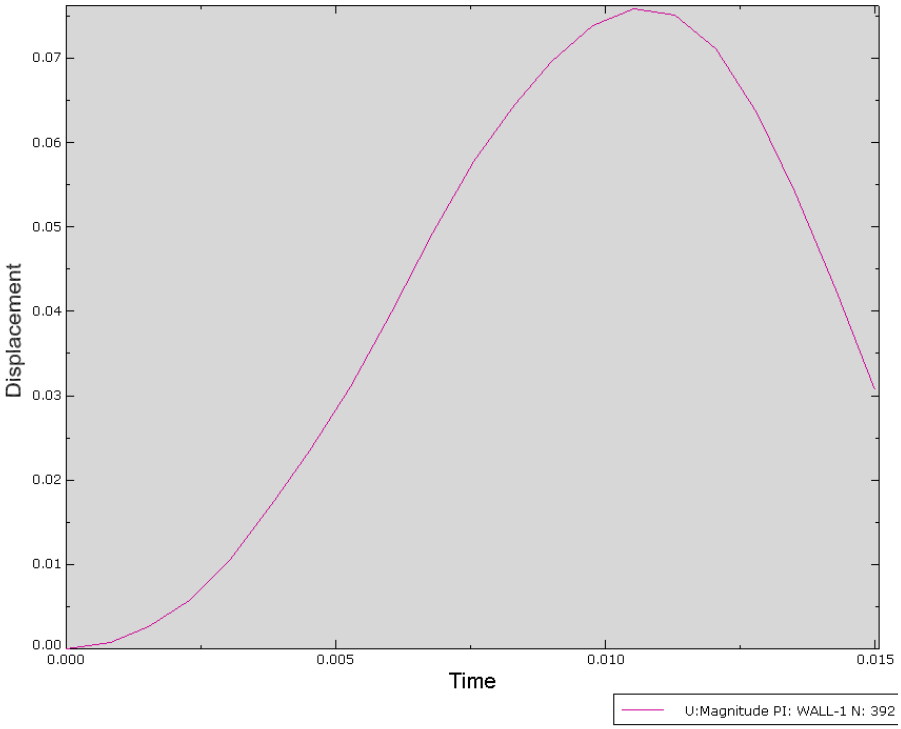

Fig. 23. Displacement vs time at the center of the wall, XY plot.

The peak of the displacement is reached after 0.01 seconds, afterwards as the time evolves the displacement decreases. As stated in the previous sentence, this behavior is due to the elastic behavior we assumed for the material model. Our intuition tells us that a displacement of that magnitude would result in a real life scenario into the cracking of the wall. This is further emphasized in the Cut View.

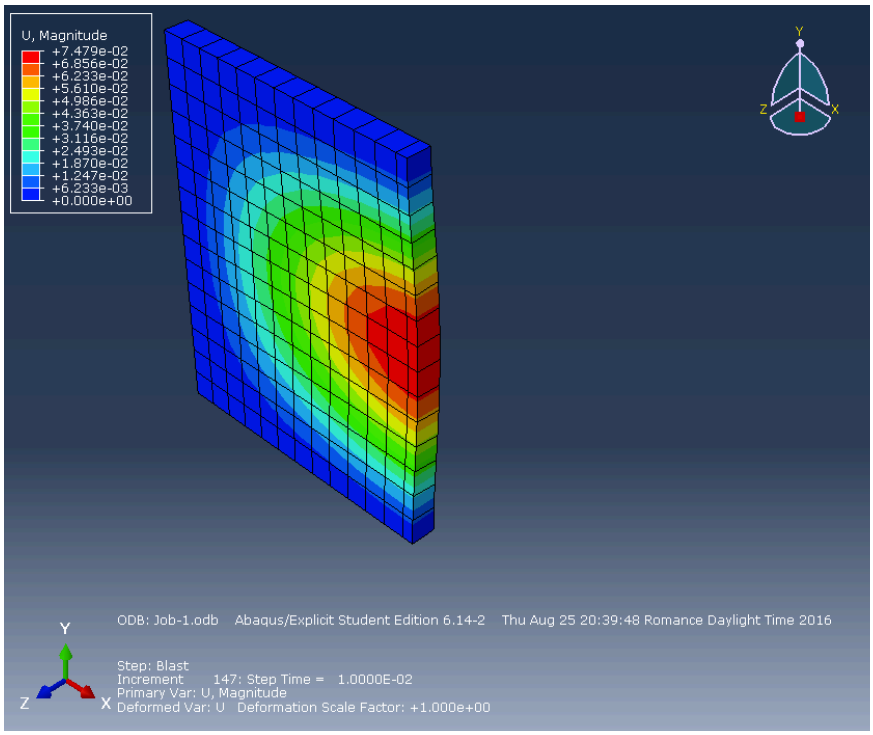

Fig. 24. Cut-View of the displacements

By clicking on activate Click View, we can observe in a more graphic manner the displacement at the center of the wall and as we continue, the 'bounce back' effect due to its elastic properties. This gives us a good idea of how the wall behaves dynamically under the blast explosion. We can observe other things such as the stress on the wall; we can see the maximum stress is present in the center of the wall.

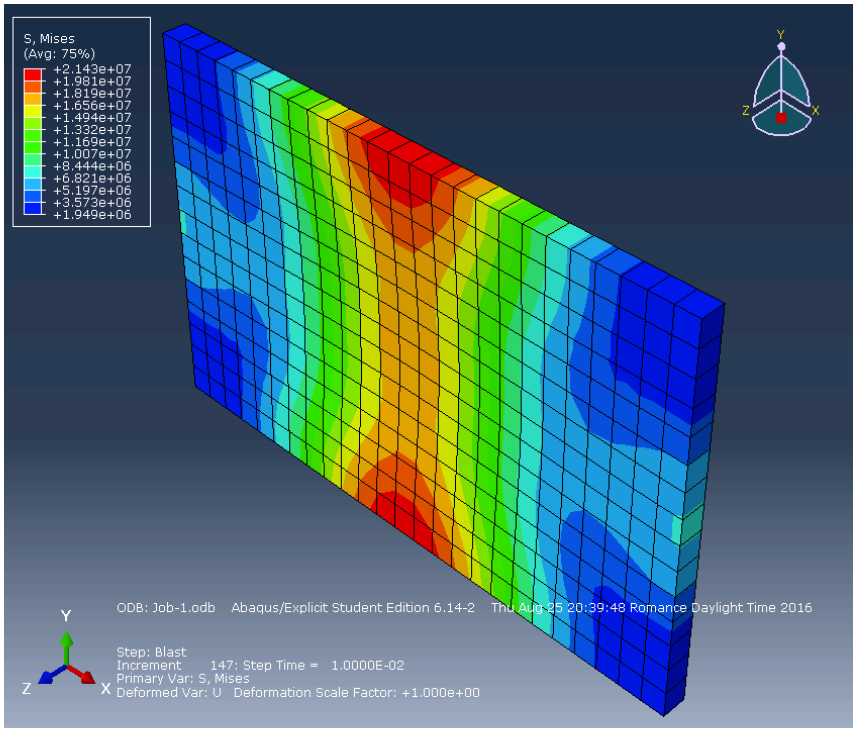

Fig. 25. Stress distribution in the masonry wall.

This first simulation, using a simple elastic model has been extremely useful. It sets our expectations for further, more complex simulations, gave us first hand on ABAQUS software and revealed some aspects of the response of the wall that will still have great importance as we progress in our study such as the stress concentration and the importance of the center node. As for now we will proceed with the next simulation using the Drucker Prager model selected in previous sections of this paper.

4.4 Mesh optimization and error estimation. In this section we present the study made in order to estimate the importance of the number of nodes used in our simulation. The ABAQUS edition used in this work is the student edition which is limited to 1000 nodes. The purpose is to estimate the differences in the results of the simulation when using a different number of nodes. The simplest way to estimate that is performing two simulations with a different number of nodes. In one simulation the approximate size of the mesh will be 0.3 meters and in the other one the size will be twice smaller. The differences between both simulations will be later analyzed and decided if the size chosen is a reasonable choice for all further simulations. In order for the reader to

appreciate visually the effect of mesh size in the simulation, two screenshots representing the mesh with 0.3 and 0.2 approximate sizes are attached:

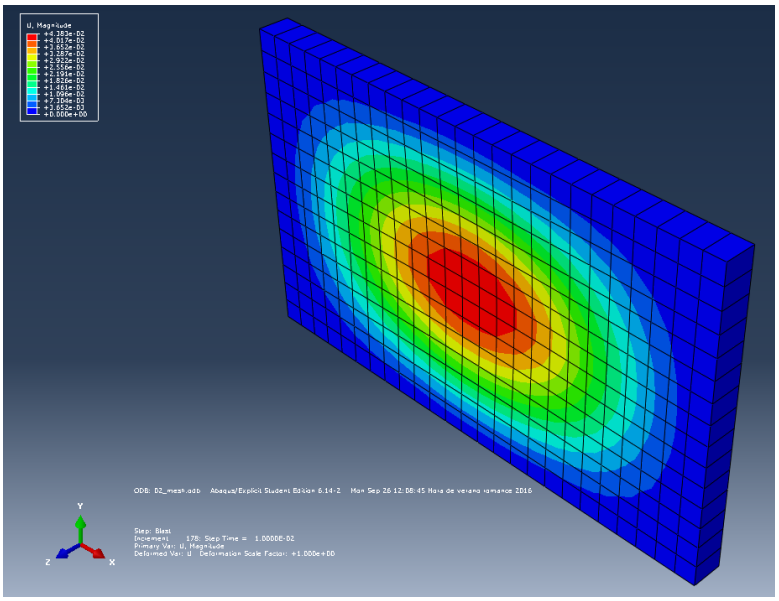

Fig. 26. Meshed figure with approx. Size of 0.2

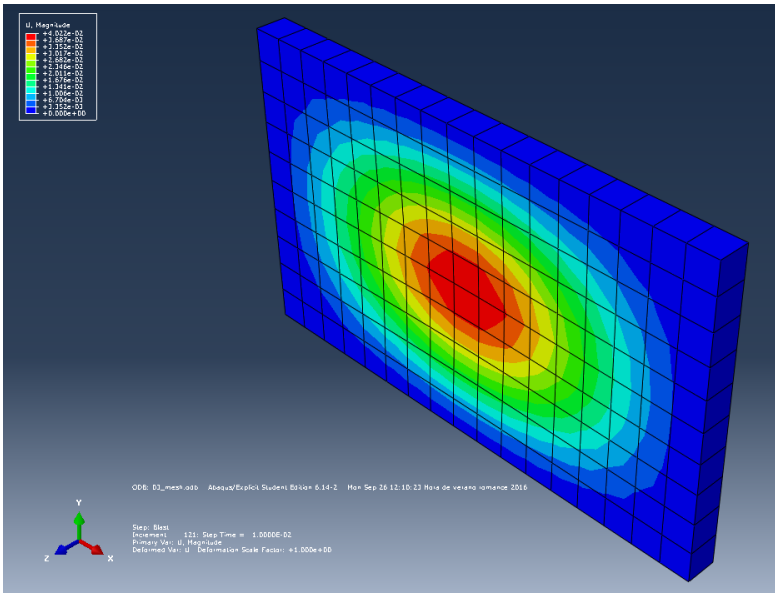

Fig. 27. Meshed figure with approx. Size of 0.3

After checking the displacement at the central node of both parts we observe an average difference between the results of 6% in terms of displacements. After analyzing the implications of this difference we can conclude that the analysis using the 0.3 approximate mesh size will provide a useful approximation of the results with

differences that, for the purpose of this paper we can tolerate. However, if a more in-depth study shall be done, we recommend the use of a Professional version for the software that will lead to more detailed and accurate simulations.

5. Implementation of the model using ABAQUS for an Unprotected Masonry Wall under explosion using a Drucker – Prager material model

5.1 Modeling the masonry wall in ABAQUS:

In this second simulation the same wall dimensions were used. For the sake of simplicity and congruence, the simulation has been submitted using the same file used in the first simulation. However, the different material model employed brings new difficulties in the discussion. First of all, we will create a new material, called Masonry – Elastic. This new material model has the same elastic properties as the previous one that was purely elastic, however the model used is the Drucker – Prager which requires new parameters. The theoretical basis for those parameters has been explained previously. We are talking about the material properties for bricks and mortar (masonry), elastic properties: density (kg/m^3), elastic modulus (N/m^2) and poisson ratio and inelastic properties: angle of friction(), flow stress ratio() and dilatation angle (). The properties used and their corresponding values were displayed in Fig. x in a previus section of this paper.

In order to finish the material model implementation, ABAQUS is also asking us for the compression hardening curve of the material. All the data has been extracted from the curve obtained by Laurenço and Roots and shown below:

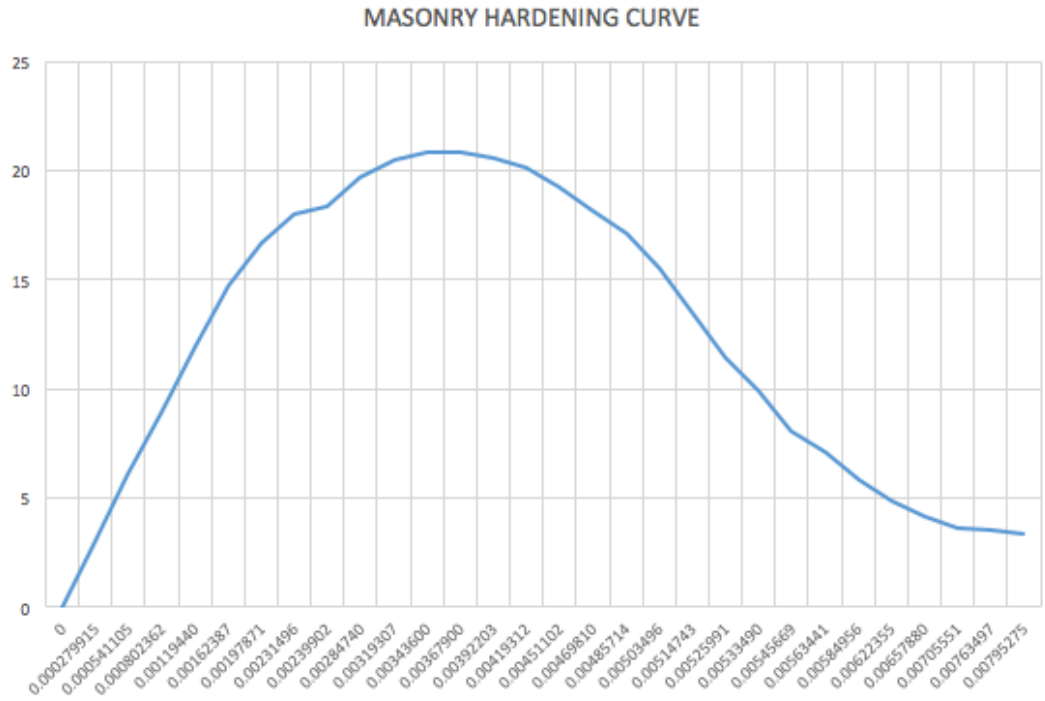

Fig. 28. Digitalized masonry curve from Laurenco.

The data found was not digitalized, so not ready to be implemented in ABAQUS. After digitizing it by hand we obtained a series of data points creating a curve similar to the one from the literature. As a next step, the data points obtained have been implemented in ABAQUS. The only part left now was assigning this newly created masonry model to the already exiting part and submitting the job for analysis.

5.2 Creating the Analysis steps:

The analysis steps are the same as in the past simulation. Everything stays basically the same in this section. However, due to a more complex material model we should expect larger computational times.

5.3 Analysis of the Results:

After the analysis is finished we head on to the results tab. Here we should pay close attention to displacements. In our simulations no damage model has been implemented in ABAQUS. In order to determine whether the wall failed or not we set our own simplified criteria. If the maximum displacement is superior to the thickness of the wall divided by two orders of magnitude, then we will consider that the wall failed under the blast explosion. The displacements are displayed in the figure below:

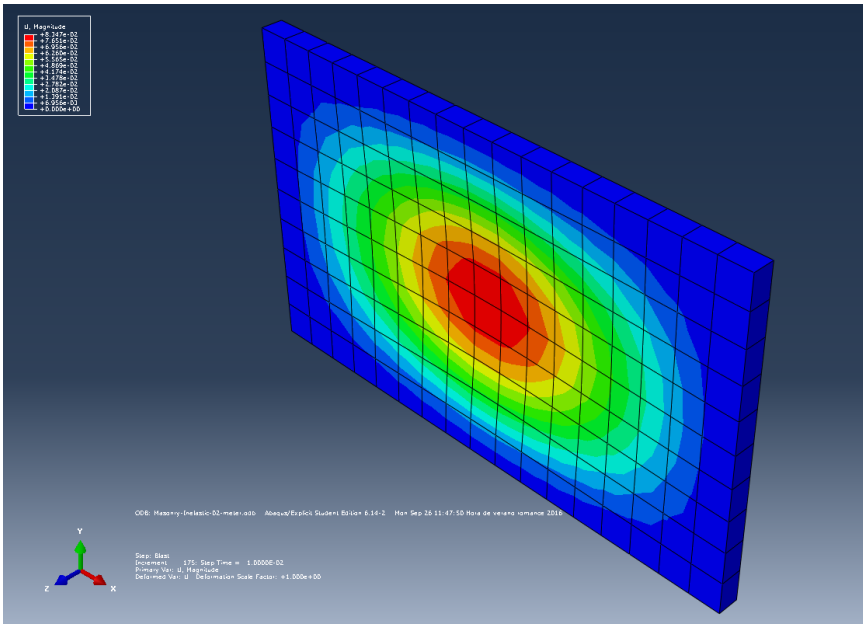

Fig. 29. Displacements in the masonry wall using Drucker-Prager criteria.

As we can see, masonry fails under the blast explosion as expected. The maximum displacement is around 8,6 centimeters, way above the threshold we set before the simulation. Those are expected results, it is indeed the purpose of this paper to avoid failure and therefore reinforce the masonry with some kind of retrofitting, in this

specific case, a natural fiber reinforced bio-composite. For in order to take a closer look at the failure, we use the cut-view:

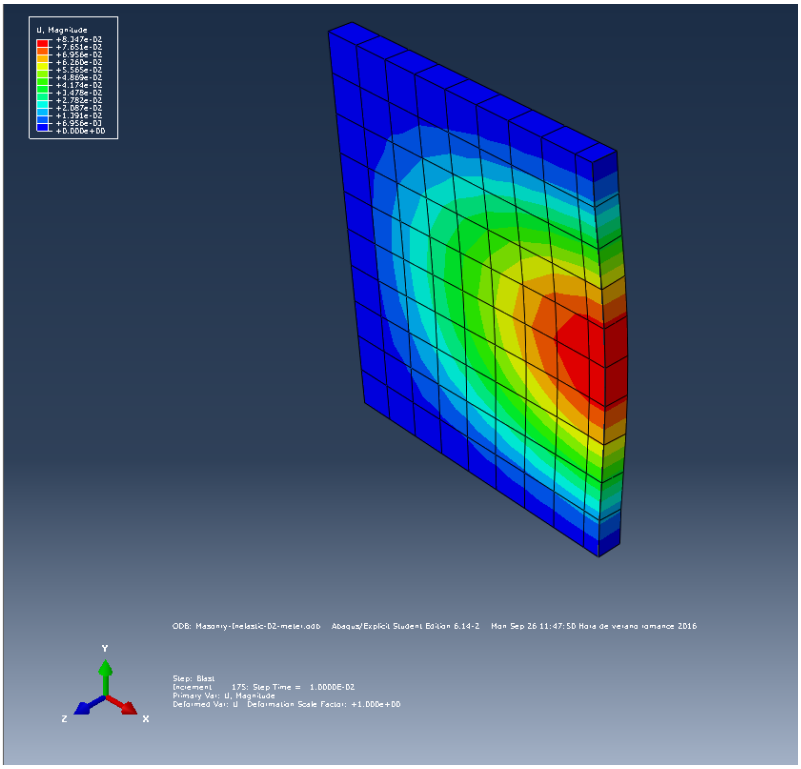

Fig. 30. Cut-view of the damaged masonry wall using Drucker-Prager strength criterion.

The displacement versus time at the node in the center of the wall is also plotted, to give and impression of the behavior of the point of maximum displacement.

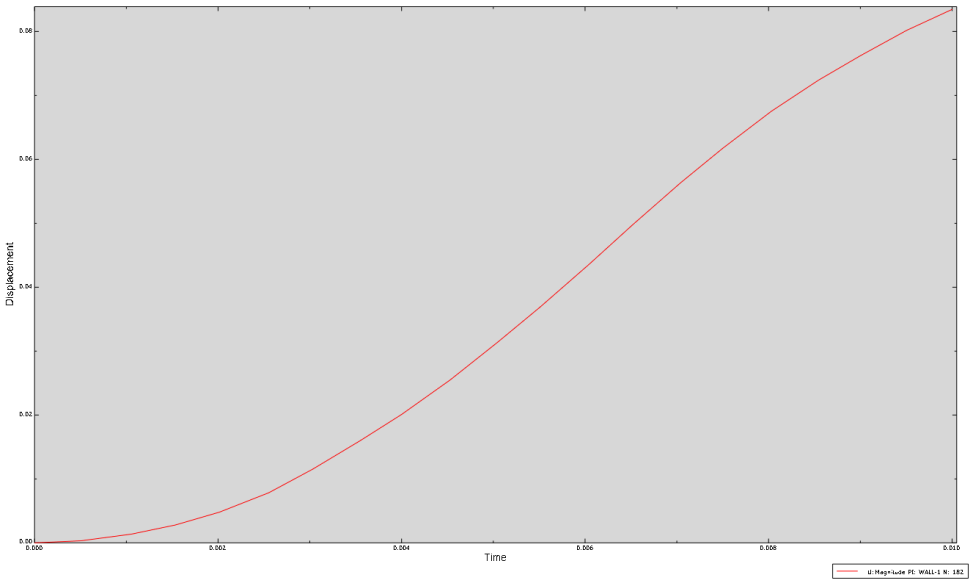

Fig. 31. Displacement versus time in the center of the wall.

Another important aspect to look at is the stress distribution. Due to the new strength criteria, we expect to see a less 'dynamic' stress distribution. The material is more brittle; we will expect a high stress concentration at the edges of the wall.

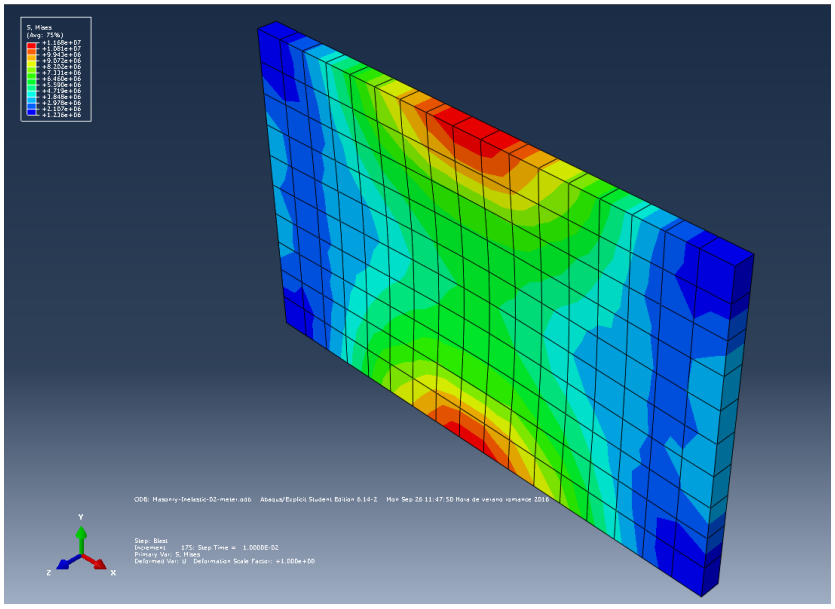

Fig. 32. Stress distribution in masonry wall with Drucker-Prager strength criteria.

As we can see in the figure above, our guess was right. There is a higher stress concentration at the borders of the wall. This is due to the less elasticity implied by the material model, which makes stress distribution harder and leads to a stress distribution. We can conclude that masonry is failing under the blast explosion if exposed without any kind of protection.

The purpose of this paper is proving that, retrofitting a masonry wall using a natural fiber reinforced bio-composite material is protective enough and more cost-effective than other traditional measures. One way to efficiently prove that is by displaying the potential save up in thickness of the wall by retrofitting it. For this purpose, the simulation has been performed for several thicknesses, the thickness of the wall has been increased gradually until the wall stopped failing under the blast explosion. The results have been displayed below:

UPROTECTED WALL			
WALL THICKNESS (m)	MAX. DISPLACEMENT (m)	FAILURE CRITERIA (m)	FAILURE
0,1	0,175320	0,001	SI
0,2	0,083585	0,002	SI

0,3	0,041022	0,003	SI
0,4	0,022447	0,004	SI
0,5	0,007131	0,005	SI
0,6	0,004631	0,006	NO

Fig. 33. Displacements and Failure in the Unprotected Masonry Wall

As we can observe, the unprotected wall keeps failing until reaching a thickness of 0.6 meters. Following our criteria, the masonry walls stops failing at that thickness and is considered reusable. For practical purposes, that thickness is not practical, especially for public or office buildings.

6. Implementation of the model using ABAQUS for a thin disposable laminate

6.1 Modeling the composite wall in ABAQUS:

The process of modeling the composite wall has some similarities with the modeling of the masonry part. However, when modeling composites, depending on the purpose of the analysis, we will find that different modeling techniques are available:

- Microscopic modeling: here, we model the matrix and the reinforcement using two separate models as deformable continuum. Afterwards, the corresponding material will be assigned to each element.
- Layered modeling: here the model will be composed of several layers, each one containing different materials.
- Smeared modeling: here, we model the composite as a homogeneous material with its own specific properties.
- Rebar modeling: this modeling technique focuses on layers of uniaxial reinforcement in surface element, particularly used to add reinforcement layers in a continuum.
- Sub-modeling: this modeling type is particularly useful when studying stress concentrations.

Besides modeling the matrix and reinforcement model, we must also define the material model, the damage and failure and the nature of the interface between both. Depending on the situation we want to model, here we find two different damage modeling techniques:

- Progressive Damage and Failure: predicts the failure modes of both matrix and fiber materials. (Hashin Criteria, UMAT, VUMAT), the Hashin criteria is the one that we will use for this simulation.
- Delamination: focuses on the separation of laminas of the composite material. (Cohesive Elements, Cohesive Contact and Virtual Crack Closure Technique)

In the case of Layered modeling, the software supports layered shell elements and layered continuum elements. In the first case, ABAQUS gives us the possibility of using two types of shells. In the first type, the conventional, only the reference surface is discretized. In the second type, the continuum, a 3D model is discretized instead. Both models can be used in modeling composites. As users, here we can define the number of layers, the material and the orientation for each layer and the section points for Simpson's integration.

In the case of layered continuum element, this feature is mainly used for example for modeling three dimensional brick elements. This capability cannot simulate shear stresses as well as the past one, but it is used as a modeling convenience. It is particularly effective when bending stresses are not of interest, not recommended in general.

Pre and Post-Processing of composite layups – the composite layup is separated in different plies. Plies usually represent uniform thickness layers of anisotropic material with fiber oriented along one reference direction. In the results section, ABAQUS offers the user the possibility of playing with plies.

After starting ABAQUS, we will begin with the implementation of the composite shell. The same dimensions as the ones for the wall are being used. The composite used in this paper is the FLA/PLAX and will have a symmetrical structure. The properties of this composite have been studied intensively in this university and are displayed below:

E1 (Gpa)	E2 (Gpa)	N12	G12	G13	G23
5	5	0.3	2	2	2

Fig. 34. Elastic properties of FLA

Xt (Mpa)	Xc (Mpa)	Yt (Mpa)	Yc (Mpa)	St (Mpa)	Sc (Mpa)
120	120	120	120	80	80
G1t (Kpa)	**G1c (Kpa)**	**G2t (Kpa)**	**G2c (Kpa)**		
432	432	432	432		

Fig. 35. Elastic properties of FLA

The Hashin failure criterion is being used for the failure of the composite. Also, the composite has been implemented in ABAQUS using the composite layup technique rather than the shell – composite material way. This will allow us a more accurate interpretation of the results.

After all the constants are introduced in ABAQUS, the simulation is ready to start. All the settings for the load (blast explosion) and the boundary conditions stay the same as in previous cases. After the analysis is finished we can start analyzing the results. The composite has been implemented in ABAQUS using the composite-layup technique. The composite layup chosen in the end has been the$[45, -45, 45, -45]_s$, with a ply thickness of 1 mm.

6.2 Analysis of the results:

To get a first impression of what is happening in this simulation, we started by plotting the displacements and the failure of the fibers in compression or torsion, finally focusing on the energy absorbed by the composite before failure. The displacements can be observed in the figure below:

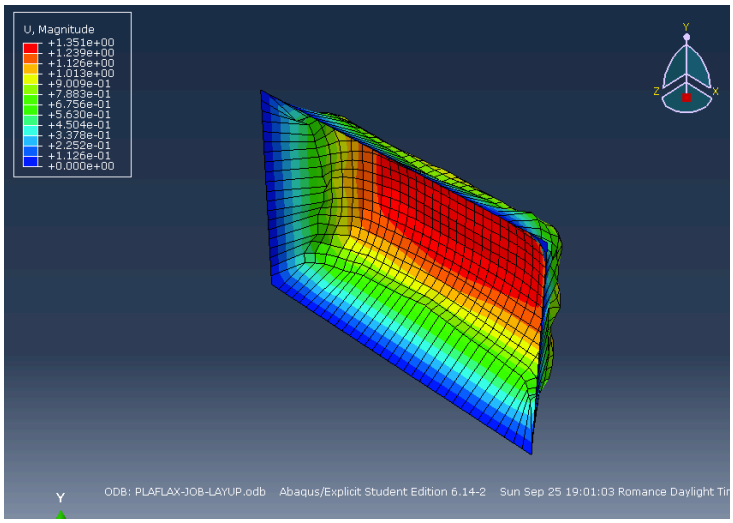

Fig. 36. Displacements in the composite coat

As we can observe, the displacements in the center of the part can reach up to 1.3 meters. This tells us that the composite layup ultimately fails under the blast explosion, matter that we have been expected counting with the mechanical properties of the composite and its thickness. In order to better illustrate the failure of the component, we plot the failure at fiber level using the Hashin criteria implemented previously. The two failure modes at the fiber level, tension and compression are plotted bellow:

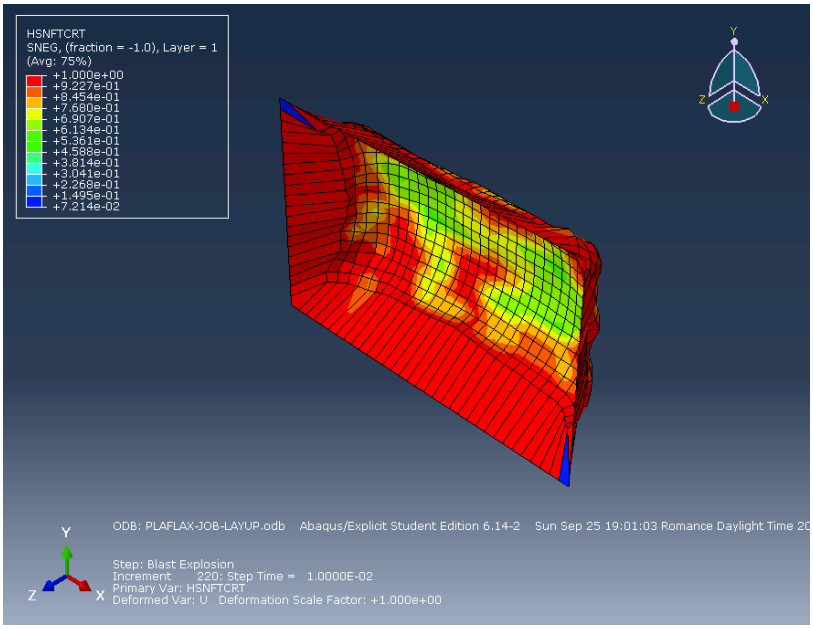

Fig. 37. Tension Hashin failure in the overall composite coat

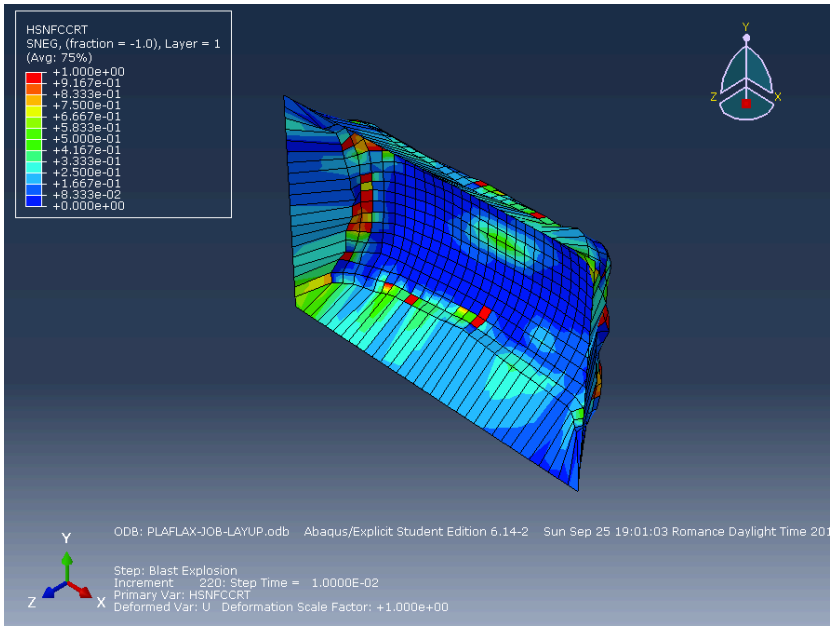

Fig. 38. Compression Hashin failure in the overall composite coat

As expected we can observe that most of fibers fail be tension, and more importantly that most fibers fail. We can also see there are some failures by compression. The fat that the composite fails under the blast explosion shouldn't worry us. As stated before, we want the composite to absorb as much energy as possible in order to avoid fragmentation and failure of the building. An interesting aspect of the failure of the composite is the failure of the various plies under different states of stress. Figures

representing the Hashin failure by tension or compression of each ply have been collected below:

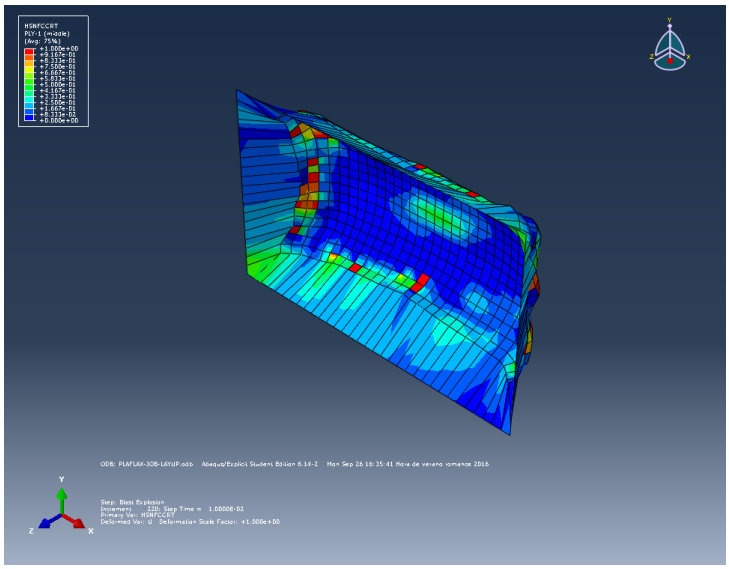

Fig. 39, Composite Ply-1 Compression Failure

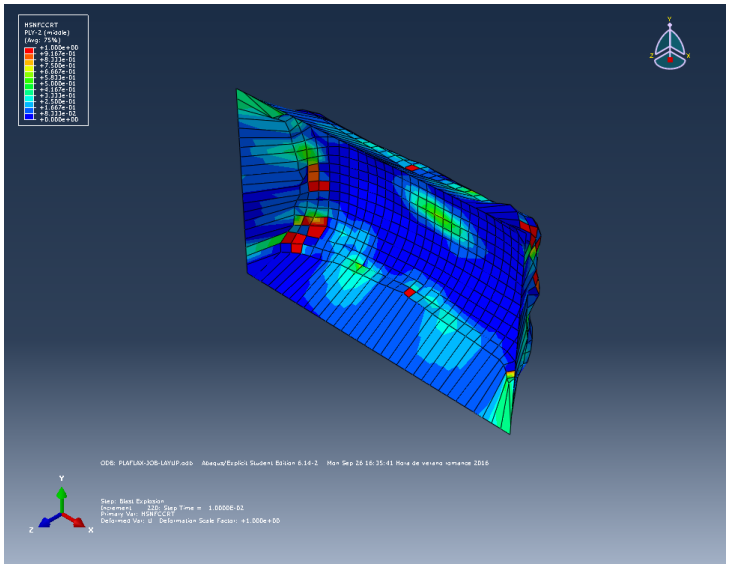

Fig. 40. Composite Ply-2 Compression Failure

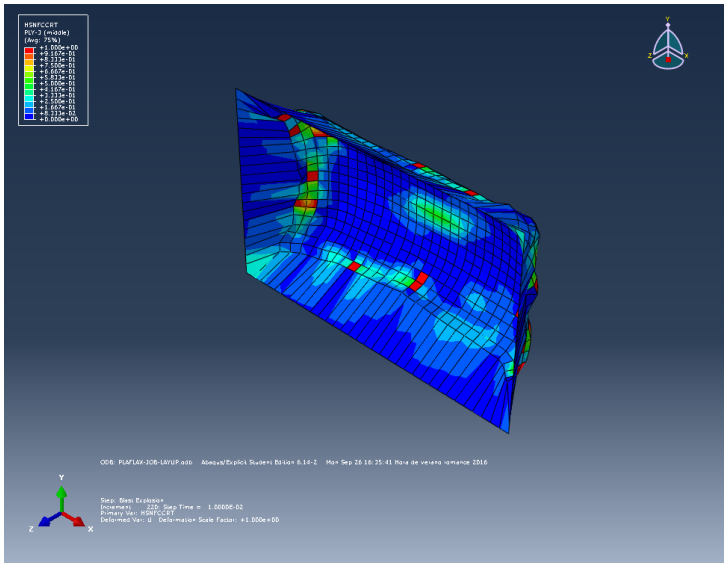

Fig. 41. Composite Ply-3 Compression Failure

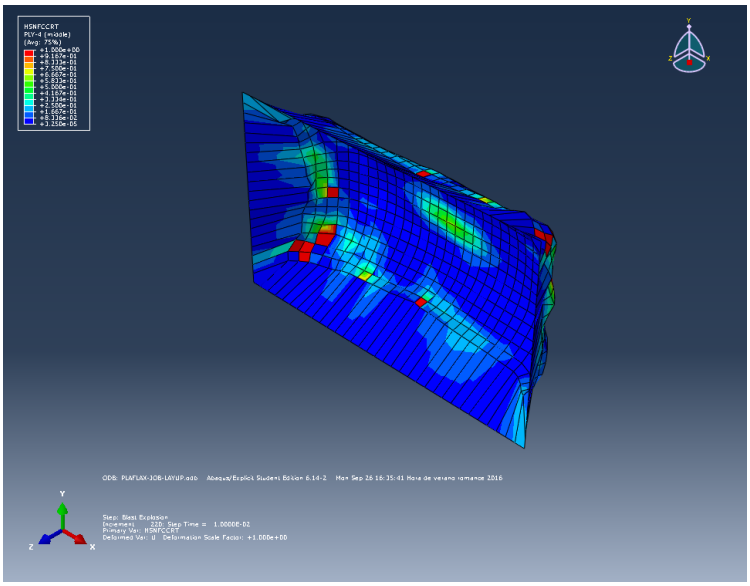

Fig. 42. Composite Ply-4 Compression Failure

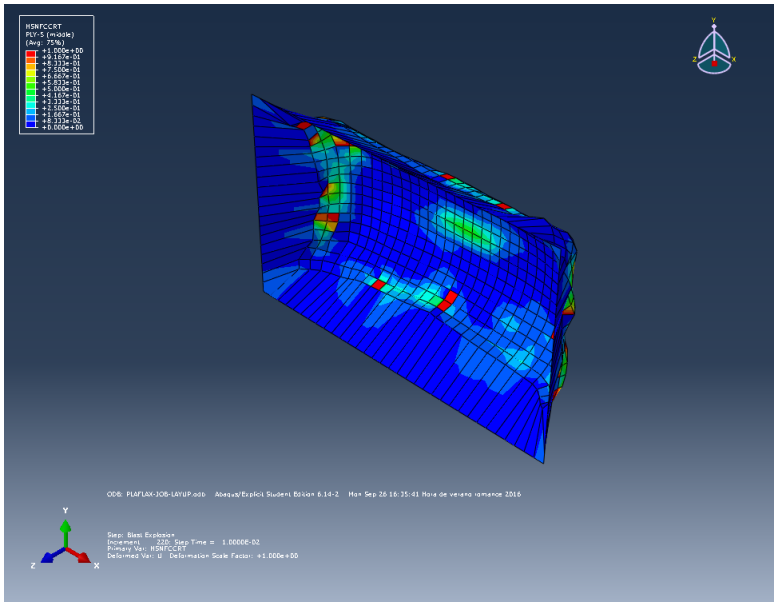

Fig. 43. Composite Ply-5 Compression Failure

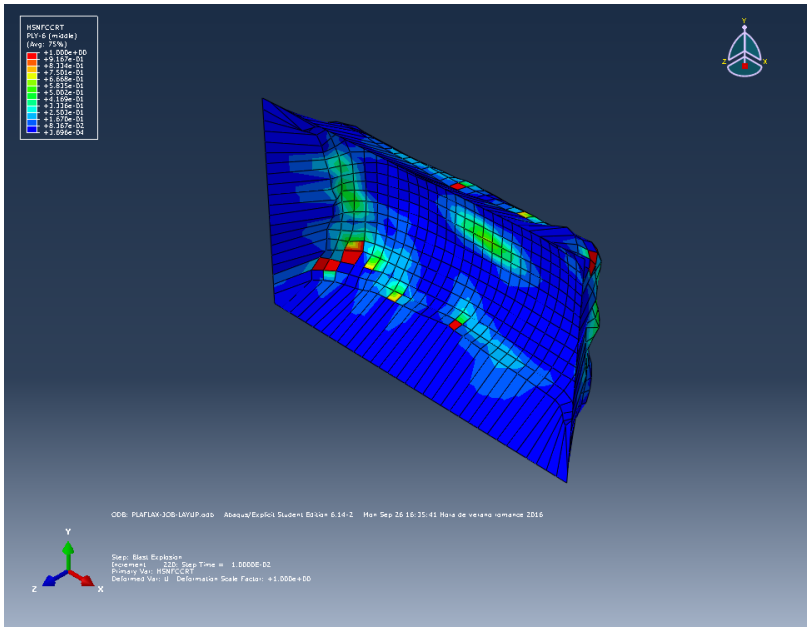

Fig. 44. Composite Ply-6 Compression Failure

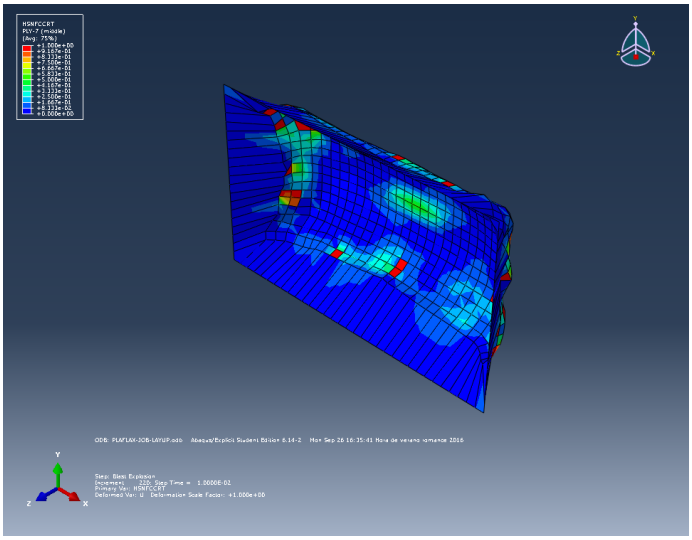

Fig. 45. Composite Ply-7 Compression Failure

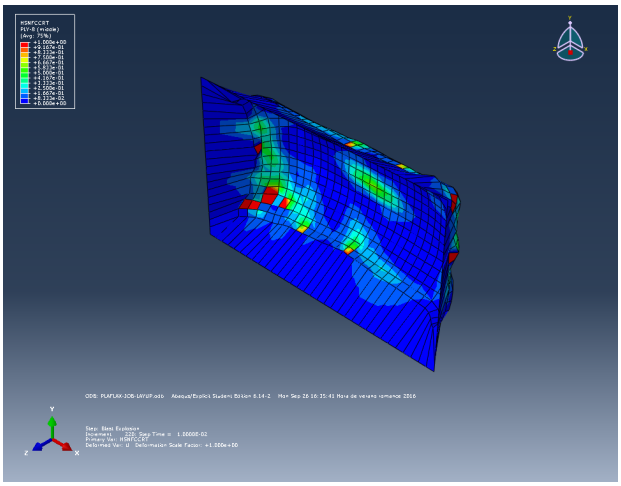

Fig. 46. Composite Ply-8 Compression Failure

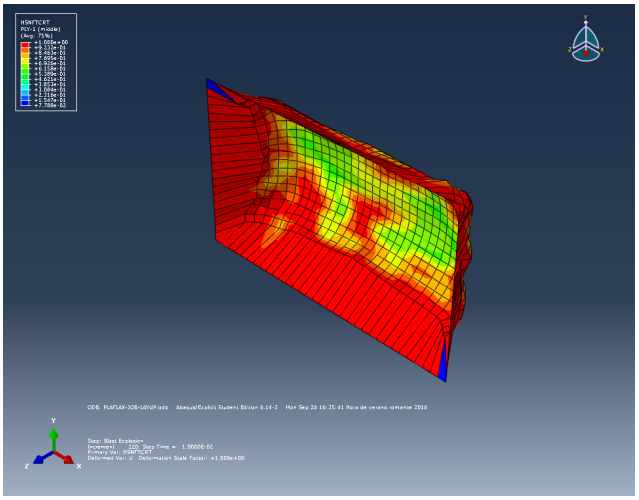

Fig. 47. Composite Ply-1 Tension Failure

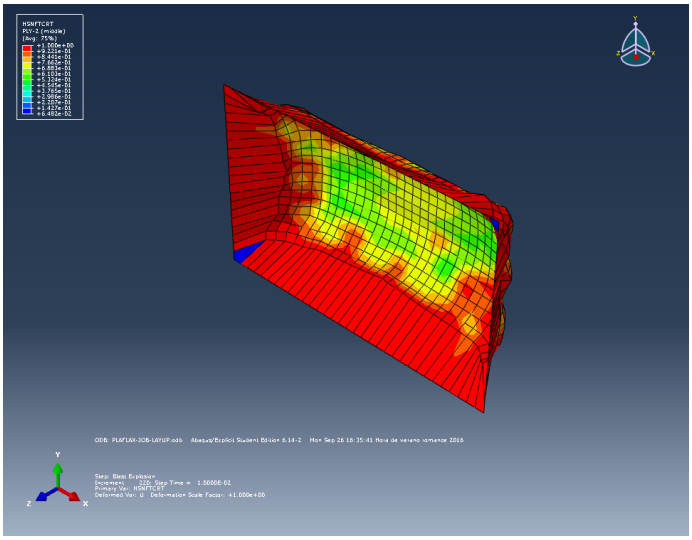

Fig. 48. Composite Ply-2 Tension Failure

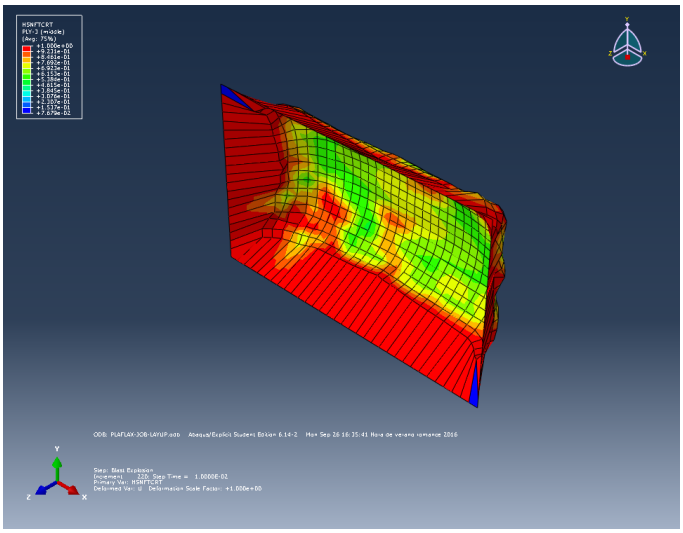

Fig. 49. Composite Ply-3 Tension Failure

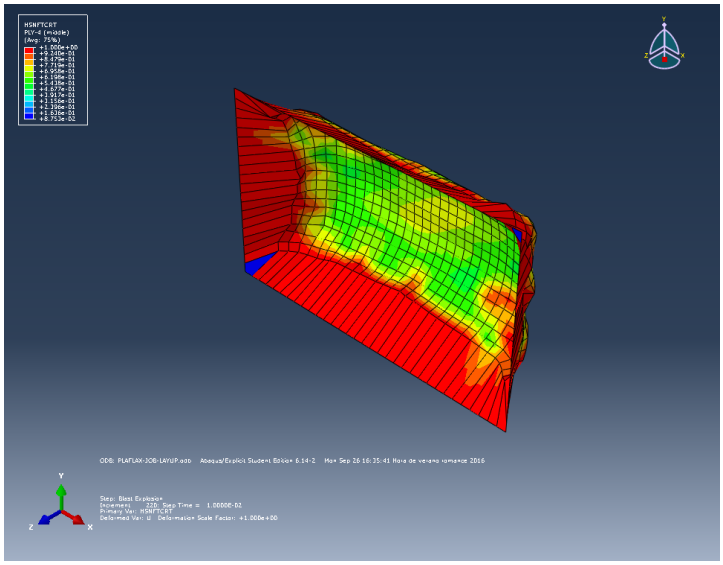

Fig. 50. Composite Ply-4 Tension Failure

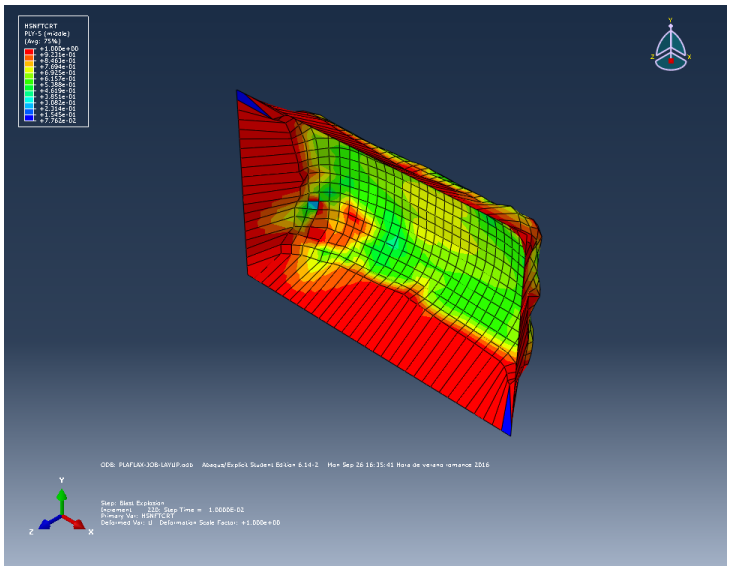

Fig. 51. Composite Ply-5 Tension Failure

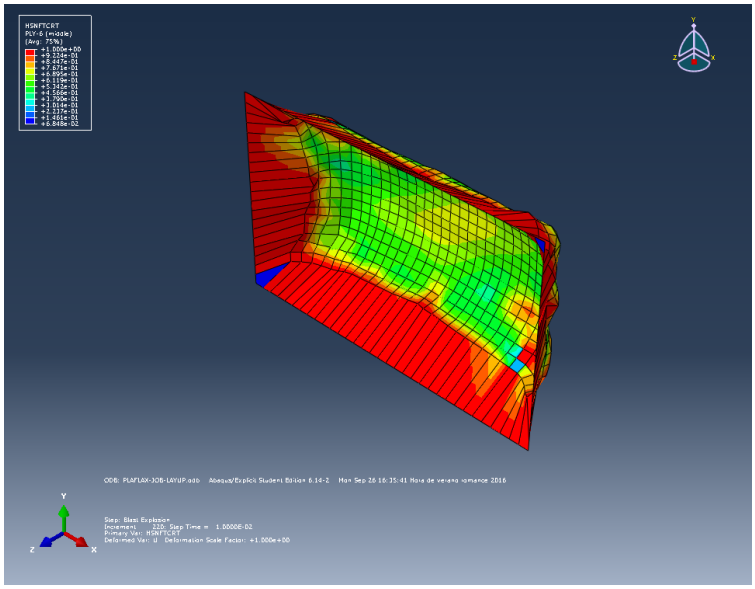

Fig. 52. Composite Ply-6 Tension Failure

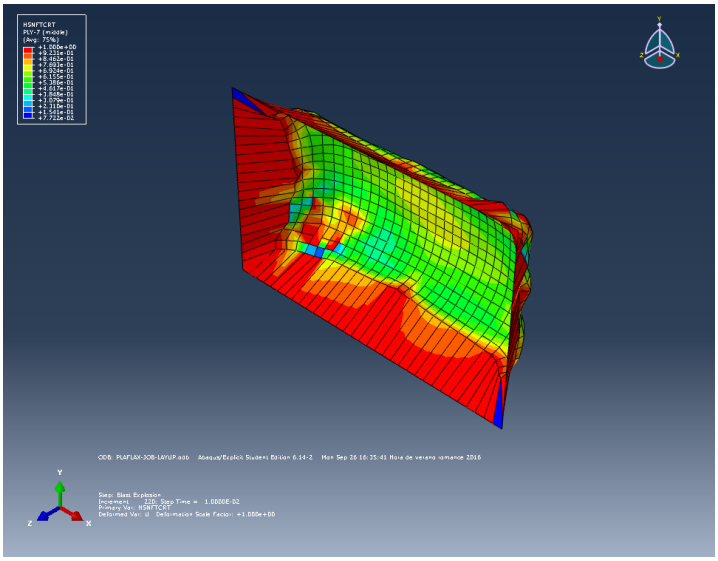

Fig. 53. Composite Ply-7 Tension Failure

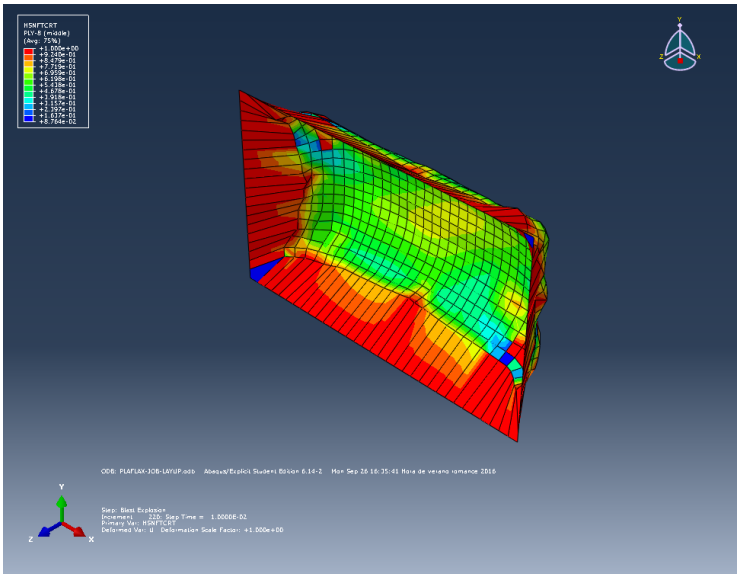

Fig. 54. Composite Ply-8 Tension Failure

As we can see in failure due to tension, the failure mode is similar. All the plies fail more or less in the same way. The behavior in compression is however interesting to discuss. Due to the loading state of the composite, some fibers located after the fibers next to the boundary conditions fail in compression mode. This is due to the 'bending' of the composite under the blast explosion which creates compression stresses at a local level.

7. Implementation, modeling and analysis of the retrofitted wall.

7.1 Modeling of the retrofitted Masonry Wall

The final simulation presented in this paper will be the simulation of the retrofitted wall. Past simulations have helped us to sense a general idea of the behavior expected. In order to clearly observe any improvement in the resistance and reusability of the wall due to the retrofitting, we will use several plots such as the kinetic energy, the displacement at the center of the wall and the failure modes. This simulation has been obtained by combining the previous simulations. The blast explosion has been simulated using the masonry wall and composite coat together and simulating the behavior for different wall thicknesses. In order to get a general idea of the simulation, the behavior of the assembly for the first simulation is displayed below:

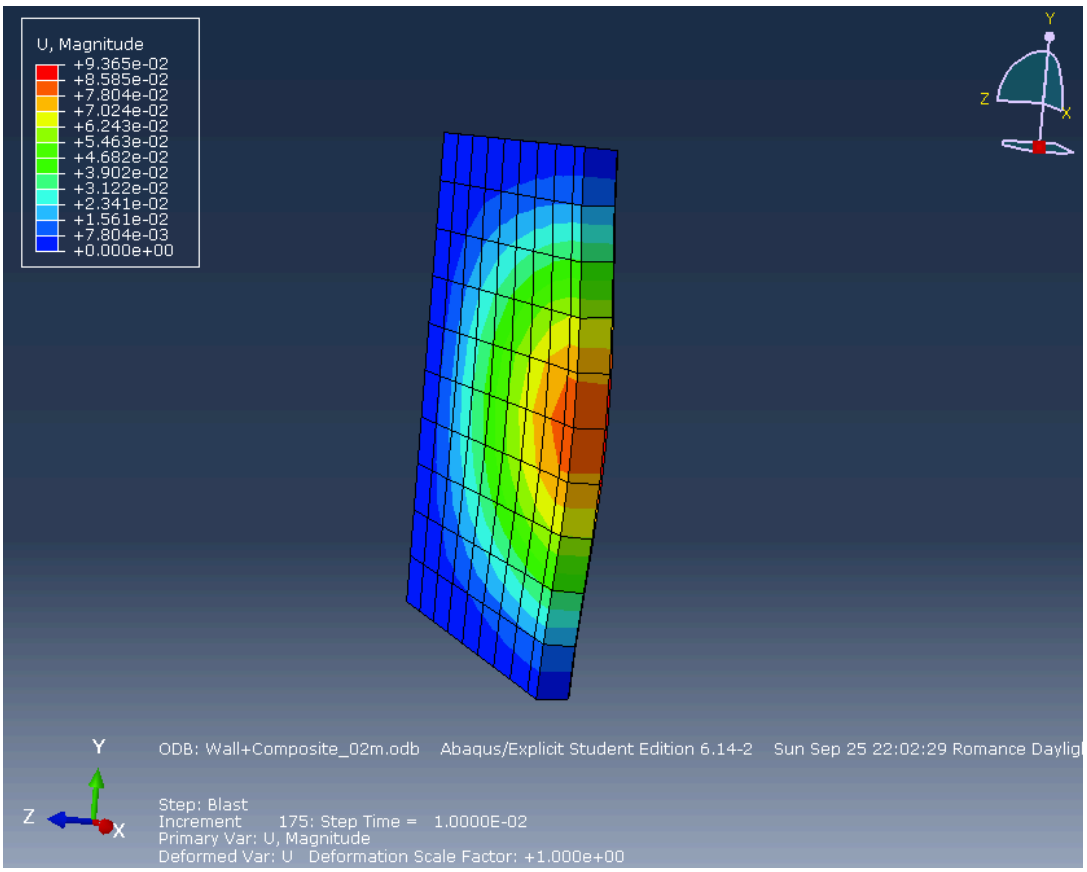

Fig. 55. Displacements and Failure in the Retrofitted Masonry Wall.

As we can observe in the figure, the composite coat absorbs energy from the wall and that leads to certain stress and strains. The distribution of stress and strain along the composite wall is follows the same patterns as in the masonry wall. In order to provide a better understanding of the interaction between both a more in-detail view is provided:

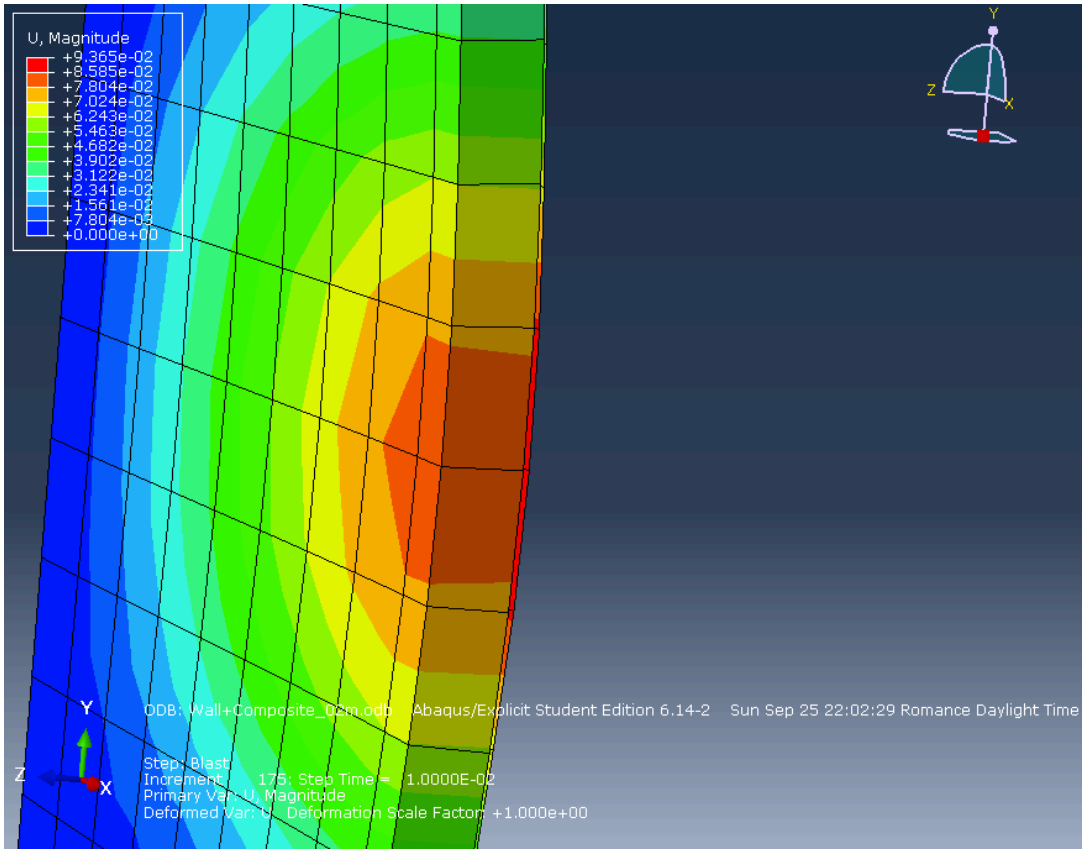

Fig. 56. Detail of displacements and Failure in the Retrofitted Masonry Wall.

In order to detect if any improvement has been achieved with the use of the composite coat, the same simulations made before with the unprotected wall have been repeated, now including the composite coat in the simulation.

7.2 Analysis of the results

The results obtained together with a comparison between protected and unprotected displacements have been provided:

RETROFITTED WALL			
WALL THICKNESS (m)	MAX. DISPLACEMENT (m)	FAILURE CRITERIA (m)	FAILURE
0,1	0,168396	0,001	SI
0,2	0,082180	0,002	SI
0,3	0,040845	0,003	SI
0,4	0,021765	0,004	SI
0,5	0,007086	0,005	SI
0,6	0,004606	0,006	NO

As we can appreciate in the figure above, the improvement provided by the composite coat is close to zero. In order to appreciate better the effects of the composite retrofitting, we will compare the maximum displacements observed in both, the unprotected and the retrofitted masonry wall:

Decrease in Max. Displacement	
Wall Thickness (m)	%Observed Improvement
0,1	3,9%
0,2	1,7%
0,3	0,4%
0,4	3,0%
0,5	0,6%
0,6	0,5%
Average Decrease in MAX. DISP.	1,7%

At first sight we may reach the conclusion that the improvement obtained by the composite coating is not considerable, that the solution might not be enough. This improvement is too small, considering the purpose of the coating. In order to get a better feeling of what is happening; several additional simulations have been made.

The first idea was to increase by an order of magnitude the number of plies in the composite. The simulation of a masonry walls with a thickness of 0,6 meters and a composite coating composed by 80 plies has been initiated. It should be noted that this simulation is orientated and has no practical meaning. A composite coat of 80 plies would not be easy to apply to the wall, and other effects, such as the interaction between plies should be taken in account when simulating it. However due in part to the limitations of the software (ABAQUS Student Edition) and the purpose of this paper, we will not advance further on. After the simulation is over, we take a look to the displacements and the energy absorbed by the composite:

RETROFITTED WALL - 80 PLIES			
Wall Thickness	Max. Displacement	%Improvement respect to 8 plies	%Improvement respect to Unprotected
0,6	0,004391	4,67%	5,18%

The improvement observed is higher than in previous cases. The decrease in thickness that we can allow due to this 5% improvement of the composite coat is not enough for our purposes. One thing we realized during those simulations is that further research in this direction should focus on the definition of a function that would relate the energy

absorption of the coating with the decrease in thickness that can be allowed in the masonry wall.

8. Conclusions and Future Work

After the several simulations of the masonry alone, the composite coat and the retrofitted masonry wall, we can reach to the conclusion that the solution presented in this paper is, at least for the moment not viable. The improvement made in the resistance of the wall, judged in terms of maximum displacement decrease and energy absorbed is not enough for this to be a considered a viable solution for the future.

However, after the research done for this paper, especially in the field of bio-composites and considering the actual situation at a global level, it should be noted that bio-degradable composites represent the only viable solution for the distant future, including blast explosion armor applications. In order for those ideas to take shape and turn into real technologies and value prepositions, research (and by research meaning funding) should be accelerated in the field, making it more attractive for researchers.

About the simulations and the work presented in this paper, several indications for the future that might increase the odds of success are presented. First of all, starting from the beginning if more time would be dedicated to recompiling the latest advances in the bio-composites field, it would result in a more proper choice for the composite. In our case the composite choice is made due to the extensive research made by our University with that kind of composite. Second of all, in terms of software and computational power, a full version of ABAQUS, not limited to 1000 nodes such as the student edition, would have improved significantly the results obtained and the flexibility of the simulations. More comparisons with solutions alike might have been possible and a more in-depth study of the masonry and the composite would have been possible.

In terms of the material model, for masonry if better results are expected a micro-modelling technique might be the most indicated. Counting with the details of the interaction between the bricks and mortar and the effects of the blast at a local level, such as micro-cracks and macro-cracks would lead to more accurate results in the simulation. Those solution, even if in the short-term might be more costly due to the high cost of experimental blast explosion and the difficulty of discretizing masonry will pay on the long term due to their eco-friendly nature and their cost-effectiveness.

9. Bibliography

1. A Review of Natural Fibers Used in Biocomposites: Plant, Animal and Regenerated Cellulose Fibers, Sunil Kumar Ramamoorthy, Mikael Skrifvars & Anders Persson (2015) A Review of Natural Fibers Used in Biocomposites: Plant, Animal and Regenerated Cellulose Fibers, Polymer Reviews, 55:1, 107-162, DOI: 10.1080/15583724.2014.971124.
2. COMPUTATIONAL STRATEGIES FOR MASONRY STRUCTURES – Paulo B. Lourenco, January 1996.
3. Electronic Guide – Manual for the Calculation of elastic Plastic Materials Models Parameters. National Physical Laboratory.
4. NUMERICAL ANALYSIS OF OUT-OF-PLANE LOADED MASONRY WALL USING HOMOGENIZATION TECHNIQUE - S. YU, C. WU, M.C. GRIFFITH - School of Civil and Environmental Engineering The University of Adelaide, SA, Australia.
5. Model validation and parametric study on the blast response of unreinforced brick masonry walls - Xueying Wei, Mark G. Stewart. Centre for Infrastructure Performance and Reliability, School of Engineering, The University of Newcastle, Callaghan, NSW 2308, Australia b School of Civil Engineering, Chang An University, Xi'an 710061, China.
6. Experimental Study on Masonry Infill Walls under Blast Loading - PEREIRA, JOÃO; CAMPOS, JOSÉ; LOURENÇO, PAULO B.
7. Finite Element Modelling of Unreinforced Masonry (URM) Wall with Openings: Studies in Australia - Department of Civil Engineering, Muhamaddiyah University, Bathoh Lueng Bata No.91, Banda Aceh, Indonesia.
8. MASONRY WALLS SUBMITTED TO OUT-OF-PLANE LOADING: EXPERIMENTAL AND NUMERICAL STUDY. Tan Trung Bui, Ali Limam, Bertrand David, Emmanuel Ferrier, Michael Brun. MASONRY WALLS SUBMITTED TO OUT-OF-PLANE LOADING: EXPERIMENTAL AND NUMERI- CAL STUDY. International Masonry Society. 8th International Masonry Conference, Jul 2010, Dresden, Germany. 2 (F-243), pp.1153-1162. <hal-00802207> .
9. Inelastic deformation and failure of profiled stainless steel blast wall panels. Part I: experimental investigations - G.S. Langdon*, G.K. Schleyer Department of Mechanical Engineering, Impact Research Centre, University of Liverpool, Brownlow Hill, Liverpool L69 3GH, UK.
10. A review on the tensile properties of natural fibre reinforced polymer composites - H Ku[+], H Wang, N Pattarachaiyakoop and M Trada, Centre of Excellence in Engineered Fibre Composites and Faculty of Engineering, University of Southern Queensland.

11. A Review on Natural Fibre Reinforced Polymer Composites C. W. Nguong, S. N. B. Lee, and D. Sujan.
12. NATURAL FIBRE REINFORCED BIODEGRADABLE POLYMER COMPOSITES J. Sahari and S.M. Sapuan.
13. Prediction of fragment size and ejection distance of masonry wall under blast load using homogenized masonry material properties - Ming Wang, Hong Hao,Yang Ding, Zhong-Xian Li.
14. Strengthening of masonry using natural fibers bonding with highly deformable adhesives - Arkadiusz Kwiecień. GSTF Journal of Engineering Technology (JET) Vol.3 No.2, July 2015.
15. Natural Fibre Bio-Composites Incorporating Poly(Lactic Acid). Eustathios Petinakis, Long Yu, George Simon and Katherine Dean.
16. A review of current development in natural fiber composites for structural and infrastructure applications - A. Ticoalu, T. Aravinthan & F. Cardona. Centre of Excellence in Engineered Fiber Composites, University of Southern Queensland Toowoomba, Australia
17. PLA Based Biopolymer Reinforced with Natural Fibre: A Review. Tapasi Mukherjee • Nhol Kao
18. COMPUTATIONAL STRATEGIES FOR MASONRY STRUCTURES: MULTI-SCALE MODELLING, DYNAMICS, ENGINEERING APPLICATIONS AND OTHER CHALLENGES - Paulo B. Lourenço. ISISE, Department of Civil Engineering School of Engineering University of Minho
19. A Simplified Model for Analysis of Unreinforced Masonry Shear Walls under Combined Axial, Shear and Flexural Loading. Bahman Ghiassi, Masoud Soltani, Abbas Ali Tasnimi
20. Analysis of building collapse under blast loads. B.M. Luccioni , R.D. Ambrosini , R.F. Danesi. Argentina.
21. Mechanical property of surface modified natural fiber reinforced PLA biocomposites. Wassamon Sujaritjun, Putinun Uawongsuwan, Weraporn Pivsa-Art, Hiroyuki Hamada.

Images:

1. http://static1.businessinsider.com/image/5171510e6bb3f71605000000-480/hurt-locker-trailer-bomb-explosion.png
2. http://wm.mbindustries.com/wp-content/uploads/2013/04/blast_clip_image002_0000.gif
3. http://www.beauregarddrywall.com/images/metal-frame/metal-framing-construction-lowell-ma-5.jpg
4. https://commons.wikimedia.org/wiki/File:Fiber-reinforced_composites_tipology.svg
5. http://www.naturalfibersforautomotive.com/wp-content/uploads/2014/04/04-mercedes-s-class-11.jpg

6. http://www.bio.miami.edu/dana/pix/cellulose_microfibrils.jpg
7. http://www.nauticexpo.com/prod/norafin/product-39320-375056.html
8. http://www.sigmaaldrich.com/content/dam/sigma-aldrich/structure2/145/mfcd00064266.eps/_jcr_content/renditions/mfcd00064266-medium.png
9. L. Averous and N.Boquillon // Carbohydr. Polym. 56 (2004) 111.
10.